Structural and behavioral analysis reveals that Insomniac impacts sleep by functioning as a Cul3 adaptor

Qiuling Li, Kayla Y. Y. Lim, and Nicholas Stavropoulos*

NYU Neuroscience Institute, Department of Neuroscience and Physiology, New York University School of Medicine, New York, NY 10016, USA

Keywords: sleep, Cullin-3, ubiquitin, ubiquitin ligase, KCTD2, KCTD5, KCTD17, myoclonic dystonia

Running Title: Structural and functional dissection of Insomniac

* **Corresponding author**

E-mail: nicholas.stavropoulos@nyumc.org

Abstract

The *insomniac* (*inc*) gene is required for normal sleep in *Drosophila* and encodes a conserved BTB protein that is a putative adaptor for the Cullin-3 (Cul3) ubiquitin ligase. Here we test whether Inc serves as a Cul3 adaptor by generating mutant forms of Inc and assessing their biochemical properties and physiological activity in vivo. We show that the N-terminal BTB domain of Inc is necessary and sufficient for Inc self-association and interactions with Cul3. Inc point mutations that weaken interactions with Cul3 impair the ability of Inc to rescue the sleep deficits of *inc* mutants, indicating that Cul3-Inc binding is critical for Inc function in vivo. Deletions of the conserved Inc C-terminus preserve Inc-Inc and Inc-Cul3 interactions but abolish Inc activity in vivo, implicating the Inc C-terminus as an effector domain that recruits Inc substrates. Mutation of a conserved C-terminal arginine similarly abolishes Inc function, suggesting that this residue is vital for the recruitment or ubiquitination of Inc targets. Mutation of the same residue in the human Inc ortholog KCTD17 is associated with myoclonic dystonia, indicating its functional importance in Inc family members. Finally, we show that Inc assembles into multimeric Cul3-Inc complexes in vivo and that depleting Cul3 causes accumulation of Inc, suggesting that Inc is negatively regulated by Cul3-dependent autocatalytic ubiquitination, a hallmark of Cullin adaptors. Our findings implicate Inc as a Cul3 adaptor and provide tools to identify the targets of Inc family proteins that impact sleep and neurological disorders.

43 **Introduction**

44 Sleep is a conserved animal behavior regulated by genetic and molecular mechanisms
45 that remain elusive. Elucidating these mechanisms is a longstanding goal in biology, given that
46 the purpose of sleep is still not well understood and because alterations in these mechanisms may
47 cause sleep disturbances, including those associated with neurodegenerative and
48 neurodevelopmental disorders. Various genes that strongly influence the duration and
49 characteristics of sleep have been identified by unbiased genetic screens in flies (Afonso et al.,
50 2015; Cirelli et al., 2005; Koh et al., 2008; Pfeiffenberger and Allada, 2012; Rogulja and Young,
51 2012; Stavropoulos and Young, 2011; Toda et al., 2019), zebrafish (Chiu et al., 2016; Singh et
52 al., 2017), worms (Iannacone et al., 2017), and mice (Funato et al., 2016). While many of these
53 genes function in pathways governing neuronal excitability or neurotransmission (Chiu et al.,
54 2016; Cirelli et al., 2005; Koh et al., 2008; Singh et al., 2017; M. Wu et al., 2014; M. N. Wu et
55 al., 2010), others influence sleep by mechanisms that remain poorly understood.

56 *insomniac* (*inc*) mutations strongly curtail the duration and consolidation of sleep but do
57 not alter its circadian regulation (Pfeiffenberger and Allada, 2012; Stavropoulos and Young,
58 2011). *inc* activity is required in neurons for normal sleep, and conversely, restoring *inc* solely to
59 neurons is largely sufficient to rescue the sleep deficits of *inc* mutants (Pfeiffenberger and
60 Allada, 2012; Stavropoulos and Young, 2011). While these findings indicate that *inc* influences
61 sleep primarily through neurons, the molecular mechanisms by which *inc* functions remain
62 poorly defined. *inc* encodes a conserved protein of the Bric-a-brac, Tramtrack, Broad Complex
63 (BTB) domain superfamily (Stavropoulos and Young, 2011), which comprises more than 80
64 proteins in *Drosophila* (Stogios et al., 2005). The BTB domain mediates protein-protein
65 interactions including homomeric self-associations and binding to heterologous proteins (Stogios

66 et al., 2005). BTB-domain containing proteins cluster into distinct subfamilies based on sequence
67 variation within the BTB domain and the presence of additional domains that underlie diverse
68 cellular functions (Stogios et al., 2005). BTB proteins include transcriptional regulators (DiBello
69 et al., 1991; Godt et al., 1993; Harrison and Travers, 1990), ion channels (Butler et al., 1989;
70 Papazian et al., 1987; Pongs et al., 1988; Wei et al., 1990), auxiliary subunits of $GABA_B$
71 receptors (Schwenk et al., 2010), and adaptors for the Cullin-3 (Cul3) ubiquitin ligase (Furukawa
72 et al., 2003; Pintard et al., 2003; Xu et al., 2003).

73 Indirect evidence suggests that Inc may serve as a substrate adaptor for the Cul3 ubiquitin
74 ligase complex (Li et al., 2017; Pfeiffenberger and Allada, 2012; Stavropoulos and Young,
75 2011). BTB proteins that function as Cul3 adaptors form homomultimers that bind Cul3 and
76 recruit substrates to Cul3 complexes for ubiquitination (Furukawa et al., 2003; Geyer et al.,
77 2003; Pintard et al., 2003; Xu et al., 2003). In cultured cells, Inc is able to bind Cul3
78 (Pfeiffenberger and Allada, 2012; Stavropoulos and Young, 2011) and to self-associate (Li et al.,
79 2017; Pfeiffenberger and Allada, 2012), but whether these molecular interactions occur in vivo
80 or are necessary for the physiological activity of Inc is unknown. Neuronal depletion of either *inc*
81 or *Cul3* causes short sleep (Pfeiffenberger and Allada, 2012; Stavropoulos and Young, 2011),
82 consistent with the notion that *Cul3* and *inc* influence sleep through a common pathway, yet the
83 modular nature of Cul3 complexes leaves unclear whether Cul3 impacts sleep through Inc. Cul3
84 assembles with tens of different BTB adaptors to ubiquitinate hundreds of substrates (Emanuele
85 et al., 2011), and may impinge upon sleep through multiple adaptor and substrate pathways. In
86 the absence of functional evidence linking Inc and Cul3 in a concerted mechanism that
87 influences sleep, the role of Inc as Cul3 adaptor remains speculative.

88 Here, we have generated mutant forms of Inc to test the hypothesis that Inc impacts sleep
89 by functioning as a Cul3 adaptor. Analysis of these Inc mutants in cultured cells and in vivo
90 reveals that Inc has the biochemical properties and molecular interactions expected of a Cul3
91 adaptor. The N-terminal BTB domain of Inc mediates interactions with Cul3 and homomeric
92 self-associations. Weakening Cul3-Inc associations impairs Inc activity in vivo, indicating that
93 Inc function requires the assembly of Cul3-Inc complexes. Deletion of the conserved C-terminal
94 domain of Inc abolishes Inc function in vivo, as does a missense mutation of a conserved,
95 disease-associated arginine residue in the C-terminal domain. These findings identify the Inc C-
96 terminus as a putative substrate binding domain and define a region within the C-terminus likely
97 to bind substrates. Mutation of the same residue in KCTD17, a human ortholog of Inc, is
98 associated with myoclonic dystonia (Mencacci et al., 2015), indicating its functional importance
99 across Inc family proteins. Our findings reveal that Inc influences sleep by functioning as an
100 adaptor for the Cul3 ubiquitin ligase complex. More broadly, our studies provide structural and
101 functional insights into Inc family proteins and tools to identify their substrates that impact
102 neuronal function and behavior.
103
104

105 **Results**

106 **The Inc BTB domain mediates Cul3 binding and Inc homomultimerization**

107 Inc and its orthologs have two conserved domains, an N-terminal BTB domain and a C-
108 terminal domain unique to Inc family members (Figures 1A and S1A) (Dementieva et al., 2009;
109 Stavropoulos and Young, 2011). The BTB domains of Cul3 adaptors mediate Cul3 binding and
110 adaptor multimerization, while distal domains recruit substrates (Furukawa et al., 2003; Geyer et
111 al., 2003; Pintard et al., 2003; Xu et al., 2003). To test whether Inc domains have the biochemical
112 properties expected of a Cul3 adaptor, we generated a deletion series in which Inc is truncated
113 progressively from its N- or C-terminus (Figure 1A). We first assessed the stability of these Inc
114 derivatives and their associations with Cul3 by expressing epitope-tagged forms of these proteins
115 in S2 cells and performing co-immunoprecipitations. Deleting residues preceding the BTB domain
116 (Inc^{22-211}) did not significantly alter interactions with Cul3 or the stability of Inc (Figure 1B). In
117 contrast, removing part of the BTB domain (Inc^{31-211}) or deleting the BTB domain entirely (Inc^{124-}
118 ^{211}) abolished Cul3 binding and resulted in a destabilized Inc protein (Figure 1B). In contrast, C-
119 terminal truncations of Inc did not alter Cul3 binding or Inc stability. Inc proteins lacking 25 C-
120 terminal residues (Inc^{1-186}), most of the C-terminal domain (Inc^{1-156}), or all residues following the
121 BTB domain (Inc^{1-123}) associated with Cul3 similarly to full-length Inc (Figure 1B), indicating that
122 the Inc C-terminus is dispensable for Inc-Cul3 interactions. The isolated Inc BTB domain (Inc^{22-}
123 ^{123}) was sufficient for Inc-Cul3 interactions, although these associations were weaker than those
124 of Inc^{1-123} (Figure 1B), suggesting that Inc N-terminal residues contribute to Cul3 binding.
125 Alternatively, weaker binding of Inc^{22-123} to Cul3 might reflect an inhibitory effect of fusing the
126 3×FLAG tag to the isolated BTB domain. Together, these results indicate that the Inc BTB domain
127 is necessary and sufficient for Cul3 binding, a key property expected of a Cul3 adaptor.

128 Next, we assessed the ability of truncated Inc proteins to associate with full length Inc.
129 Partial deletion of the Inc BTB domain (Inc^{31-211}) or its complete removal ($Inc^{124-211}$) abolished
130 Inc-Inc interactions (Figure 1C). The reduction in Inc stability caused by truncating the BTB
131 domain (Figures 1B and 1C) suggests that Inc is an obligate homomultimer and that Inc monomers
132 are intrinsically unstable. In contrast, C-terminal truncations of Inc did not detectably alter Inc-Inc
133 associations (Figure 1C), indicating that the Inc C-terminus is dispensable for Inc multimerization.
134 The Inc BTB domain (Inc^{22-123}) was sufficient to bind Inc (Figure 1C), albeit more weakly than
135 Inc^{1-123}, suggesting that N-terminal Inc residues contribute to Inc-Inc interactions or that
136 interactions of the isolated BTB domain are occluded by the 3×FLAG tag. We conclude that the
137 Inc BTB domain mediates Inc self-association and Cul3 binding and that the Inc C-terminus is
138 dispensable for these interactions.
139
140 **Identification of Inc point mutants that selectively weaken Inc-Cul3 and Inc-Inc interactions**
141 We next sought to identify Inc point mutants that selectively perturb Inc-Cul3 and Inc-Inc
142 interactions, in order to test the necessity of these interactions for Inc activity in vivo. Our efforts
143 to mutagenize Inc were informed by the crystal structure of human KCTD5, an Inc ortholog that
144 forms homopentamers (Dementieva et al., 2009), and by the structures of Cul3 complexed with
145 BTB-MATH and BTB-BACK-Kelch adaptors (Canning et al., 2013; Errington et al., 2012; Ji and
146 Privé, 2013), in which adaptors form homodimers and assemble with Cul3 in a 2:2 stoichiometry
147 (Canning et al., 2013; Errington et al., 2012; Ji and Privé, 2013). While Inc and its orthologs are
148 divergent from BTB-MATH and BTB-BACK-Kelch adaptors and likely bind Cul3 with a different
149 mechanism and stoichiometry (Balasco et al., 2014; Ji et al., 2015), comparison of these structures
150 suggested a region of Inc that may bind Cul3. We selected eight residues in the Inc BTB domain

151 that are conserved between Inc and its three human orthologs and that reside on the solvent-
152 accessible surface of KCTD5 (Figures S1A and S1B), reasoning that these residues may contribute
153 to Cul3 binding. We mutated these residues individually to alanine (F47A, D57A, D61A, F105A,
154 Y106A, N107A) or to oppositely charged residues (R50E, E104K), and assessed the consequences
155 for Inc-Inc and Inc-Cul3 interactions in cultured S2 cells. Most mutants did not detectably alter
156 Inc self-association or Cul3 binding (Table 1). Two mutants, F47A and F105A, weakened
157 interactions with Cul3 but did not significantly affect Inc self-association or stability (Figures 2A
158 and 2B). A double mutant combining F47A and F105A behaved similarly and selectively impaired
159 Cul3 binding (Figures 2A and 2B). These phenylalanine residues cluster in a hydrophobic patch
160 on the surface of KCTD5 that may be buried upon Cul3 binding (Figure S1B). This patch is distinct
161 from the interface of adjacent KCTD5 subunits, consistent with the lack of a measurable impact
162 of mutating F47 and F105 on Inc-Inc interactions (Figure 2B).

163 To identify Inc mutants that impair Inc-Inc homomultimerization, we mutated seven
164 conserved residues that form a network of polar and charged interactions between adjacent KCTD5
165 subunits (Dementieva et al., 2009) (Figures S1A and S1C). We mutated these residues to alanine
166 (T36A, D71A, D73A, N82A) or to oppositely charged residues (R85E, K88D, E101K) in single
167 and double mutant combinations. None of these single or double mutants significantly altered Inc
168 self-associations in S2 cells (Table 2). We reasoned that Inc may form homopentamers, like
169 KCTD5, and that cooperative interactions between Inc subunits might limit the effects of these
170 mutations. We therefore generated a triple point mutant predicted to disrupt interactions of Inc
171 subunits with both flanking neighbors in a putative Inc pentamer (T36A, D71A, R85E) (Figure
172 S1C). This triple mutant exhibited significantly weakened interactions with both Inc and Cul3 and
173 a markedly reduced stability (Figures 2C and 2D), resembling the consequences of deleting the

174 Inc BTB domain (Figures 1B and 1C). These findings support the conclusion that multimerization-
175 deficient Inc proteins are unstable and suggest that Inc multimerization is required for efficient
176 Cul3 binding. These results furthermore suggest that Cul3 binds cooperatively to adjacent Inc
177 subunits and that Cul3-Inc complexes have an architecture distinct from Cul3-adaptor complexes
178 formed by BTB-MATH and BTB-BACK-Kelch proteins (Canning et al., 2013; Errington et al.,
179 2012; Ji and Privé, 2013).
180

181 **The assembly of Inc-Cul3 complexes in vivo is required for the function of Inc**

182 Inc mutations that selectively impair Cul3 binding represent key tools to assess whether
183 Inc impacts sleep by functioning as a Cul3 adaptor. To assess the physiological activity of Inc
184 mutants in vivo, we generated UAS transgenes expressing 3×FLAG-Inc or -Inc point mutants that
185 weaken Cul3 interactions: Inc^{F47A}, Inc^{F105A}, and $Inc^{F47A/F105A}$. We integrated these transgenes at the
186 same genomic site (*attP2*) and backcrossed them to generate an isogenic allelic series, enabling
187 careful comparisons of their activity. We first assessed the expression of these proteins using *inc-*
188 *Gal4*, a driver that fully rescues the sleep deficits of *inc* mutants when used to restore *inc*
189 expression (Li et al., 2017; Stavropoulos and Young, 2011) and which therefore recapitulates *inc*
190 expression in cells relevant for sleep. Inc and Inc point mutants were expressed at similar levels
191 under *inc-Gal4* control in *inc* mutants (Figure 3A) or inc^{+} animals (Figure S2A), indicating that
192 these point mutants do not alter Inc stability in vivo, recapitulating findings from cultured cells
193 (Figures 2A and 2B). Next, we assessed the impact of expressing Inc point mutants on sleep-wake
194 behavior. Because adaptor proteins deficient for Cul3 interactions might sequester substrates and
195 thus function as dominant negatives, we first tested whether the sleep of inc^{+} animals was altered
196 by the expression of Inc point mutants. Animals expressing Inc point mutants under the pan-

197 neuronal *elav*^{c155}*-Gal4* control slept indistinguishably from those expressing wild-type Inc and
198 from control animals lacking *UAS* transgenes (Figure S2B). Thus, expression of Inc point mutants
199 in neurons does not elicit dominant negative effects or antagonize endogenous Inc function.

200 We next tested whether Inc-Cul3 interactions are required for Inc function in vivo. If so,
201 attenuating these interactions should impair the ability of Inc to rescue the sleep phenotypes of *inc*
202 mutants. While Inc expressed with *inc-Gal4* fully rescued the short sleep of *inc*^{1} null mutants, Inc
203 mutants that weaken Inc-Cul3 interactions provided only a partial rescue (Figures 3B and 3C),
204 supporting the interpretation that Inc activity in vivo requires binding to the Cul3 ubiquitin ligase
205 complex. Rescue was more strongly impaired for Inc^{F105A} and Inc$^{F47A/F105A}$ than Inc^{F47A} (Figures
206 3B and S3A-D). Because these Inc mutants are expressed at similar levels in vivo (Figure 3A), we
207 speculate that the F47A mutation might impair Cul3 binding in vivo to a lesser degree than in S2
208 cells. Collectively, the impaired rescuing activity of this trio of Inc mutants suggests that Inc
209 activity requires the assembly of Cul3-Inc complexes in vivo and that disruption of these
210 complexes inhibits sleep.

211

212 **The conserved C-terminal domain of Inc is essential for Inc activity in vivo**

213 While the Inc C-terminus is dispensable for Inc-Inc and Inc-Cul3 associations (Figures 1B
214 and 1C), its evolutionary conservation suggests an essential function. If Inc serves as a Cul3
215 adaptor, its C-terminus is predicted to bind substrates and recruit them to the Cul3 complex for
216 ubiquitination. To test whether the C-terminus is required for physiological function of Inc in vivo,
217 we generated *UAS* transgenes expressing 3×FLAG-tagged Inc C-terminal truncations: Inc$^{1-186}$,
218 Inc$^{1-156}$, and Inc$^{1-123}$. These proteins were expressed at similar levels under *inc-Gal4* control in *inc*
219 mutants (Figure 4A), indicating that these proteins are stable in vivo, as in cultured cells (Figures

220 1B and 1C). Neuronal expression of Inc C-terminal truncations using *elav*^{c155}*-Gal4* did not
221 significantly alter sleep, indicating that these proteins do not elicit dominant negative effects or
222 antagonize endogenous *inc* function (Figure S4).

223 To determine whether the Inc C-terminus is essential for Inc function, we tested whether
224 C-terminally truncated Inc proteins rescue the sleep deficits of *inc* mutants. Wild-type Inc
225 expressed under *inc-Gal4* control fully rescued the sleep deficits of *inc*^{1} mutants (Figures 4B and
226 4C). In contrast, animals expressing Inc$^{1-156}$ or Inc$^{1-123}$ slept indistinguishably from *inc* mutants,
227 indicating that these proteins failed to rescue the *inc* phenotype (Figures 4B and 4C). Expression
228 of Inc$^{1-186}$ partially rescued the sleep phenotypes of *inc* mutants as assessed by several sleep
229 parameters, including total sleep duration (Figure 4B), nighttime and daytime sleep (Figures S5A
230 and S5B), and sleep bout duration and number (Figures S5C and S5D). These findings indicate
231 that the Inc C-terminus is essential for Inc activity in vivo and that removing the terminal 25
232 residues of Inc curtails Inc function. The stability of C-terminally truncated Inc proteins and their
233 ability to engage normally in Inc-Cul3 and Inc-Inc interactions (Figures 1B and 1C), supports the
234 hypothesis that the Inc C-terminus recruits Inc binding partners including substrates whose
235 ubiquitination influences sleep.

236

237 **Mutation of a conserved disease-associated arginine in the Inc C-terminus abolishes Inc**
238 **function and defines a region of Inc likely to recruit substrates**

239 To further dissect the function of the Inc C-terminus, we mutated several conserved
240 residues whose attributes suggested they might contribute to Inc function. A missense mutation of
241 a conserved C-terminal arginine in the human Inc ortholog KCTD17 (R145H) is associated with
242 a dominant form of myoclonic dystonia, a neurological movement disorder (Mencacci et al., 2015).

243 We reasoned that this arginine residue might be critical for the function of Inc and its orthologs.
244 In particular, the analogous residue in KCTD5 (R159) resides on a lateral solvent-accessible
245 surface of the C-terminal domain that might bind and orient substrates for Cul3-dependent
246 ubiquitination (Figure S1D). We therefore generated the analogous mutation in Inc (Inc^{R135H}) to
247 assess whether it impacts Inc function. We also mutated three conserved Inc residues (N167, Y168,
248 G169) to alanine (Inc^{AAA}), reasoning that their location within a surface-exposed loop on the
249 bottom surface of the KCTD5 C-terminus and their conservation amid flanking non-conserved
250 residues (Figures S1A and S1D) might reflect an important function. In cultured S2 cells, both
251 Inc^{R135H} and Inc^{AAA} were stably expressed and associated with Cul3 and Inc indistinguishably from
252 wild-type Inc, indicating that these mutations do not alter Inc multimerization or Cul3 binding
253 (Figure 5).

254 To determine whether Inc^{R135H} and Inc^{AAA} alter the physiological activity of Inc, we
255 generated UAS transgenes to express these mutants in vivo. As in cultured cells, Inc^{R135H} and
256 Inc^{AAA} were stably expressed in vivo (Figure 6A). Expression of Inc^{R135H} and Inc^{AAA} with *elav*^{c155}-
257 *Gal4* did not alter sleep in *inc*$^{+}$ animals, indicating that these proteins do not have dominant
258 negative activity or inhibit endogenous Inc function (Figure S6). Next, we tested whether Inc^{R135H}
259 and Inc^{AAA} were able to rescue the sleep deficits of *inc* mutants. Inc^{R135H} was unable to restore
260 sleep to *inc*^{1} mutants, indicating that the R135H mutation abolishes Inc function (Figures 6B-C
261 and S7A-D). In contrast, Inc^{AAA} completely rescued *inc*^{1} mutants and behaved indistinguishably
262 from wild-type Inc (Figures 6B-C and S7A-D). These data indicate that R135 is critical for Inc
263 function and suggest that mutation of this residue impairs the recruitment of Inc binding partners
264 including substrates. The analogous mutation in KCTD17 may similarly alter its ability to engage

265 targets, suggesting that deficient substrate ubiquitination is a cause of KCTD17-associated
266 myoclonic dystonia.
267
268 **Inc exhibits properties of a Cul3 adaptor in neurons in vivo**
269 Neuronal depletion of *inc* or *Cul3* shortens sleep, indicating that the activity of both genes
270 is required in neurons for normal sleep (Pfeiffenberger and Allada, 2012; Stavropoulos and Young,
271 2011). We performed a series of experiments to determine whether Inc exhibits the properties of
272 a Cul3 adaptor in vivo. First, we tested whether Cul3-Inc complexes assemble in vivo, by co-
273 expressing epitope-tagged Inc and Cul3 in neurons using the *elav*^{c155}*-Gal4* driver and performing
274 co-immunoprecipitations. We observed that Cul3 and Inc associate in neurons in vivo (Figure 7A).
275 Second, we tested whether Inc homomultimerizes in vivo, by co-expressing HA-Inc and Myc-Inc
276 in neurons and assessing their physical interactions. We observed strong self-association of Inc in
277 neurons (Figure 7B), indicating that Inc forms homomultimeric complexes in vivo, as in cultured
278 cells (Figure 1C) (Li et al., 2017; Pfeiffenberger and Allada, 2012). Third, we tested whether Inc
279 abundance is regulated by Cul3 in vivo. Cul3 adaptors are often regulated by autocatalytic
280 ubiquitination and degradation in Cul3 complexes (Djagaeva and Doronkin, 2009; Geyer et al.,
281 2003; Hudson and Cooley, 2010; Pintard et al., 2003; Wee et al., 2005; Zhang et al., 2005). To test
282 whether Inc abundance is regulated by Cul3 activity, we expressed neuronal RNAi against *Cul3*
283 and assessed Inc levels in head lysates. We observed an increase in Inc protein levels upon
284 depletion of Cul3 (Figure 7C), indicating that Cul3 negatively regulates Inc in adult neurons. qRT-
285 PCR revealed that neuronal Cul3 RNAi did not increase *inc* transcript levels, indicating that
286 elevated Inc levels arise by a post-transcriptional mechanism (Figure 7D). We conclude that Inc is
287 regulated endogenously in neurons by Cul3-dependent autocatalytic ubiquitination and subsequent

288 degradation. Together, these results indicate that Inc binds Cul3 in vivo and has the characteristics
289 expected of a Cul3 adaptor in neurons, a cell type through which *inc* influences sleep
290 (Pfeiffenberger and Allada, 2012; Stavropoulos and Young, 2011).
291

292 **Discussion**

293 The neuronal activity of Insomniac is vital for sleep, yet the molecular mechanism
294 underlying its function has remained speculative. Our analysis implicates Inc as a Cul3 adaptor in
295 vivo and provides insight into the mechanism by which Inc binds Cul3 and recruits substrates to
296 ultimately impact behavior. Inc has a modular organization and conserved domains that fulfill the
297 properties expected of a Cul3 adaptor (Furukawa et al., 2003; Geyer et al., 2003; Pintard et al.,
298 2003; Xu et al., 2003). The Inc BTB domain mediates the homomeric assembly of Inc and
299 interactions with Cul3, while the Inc C-terminus is dispensable for these interactions but is vital
300 for Inc function in vivo, consistent with its putative function in recruiting substrates to Cul3-Inc
301 complexes for ubiquitination. Inc assembles into Cul3-Inc complexes in neurons and importantly,
302 reducing the affinity of Inc-Cul3 associations impairs the activity of Inc in vivo. These findings
303 link the biochemical associations of Cul3 and Inc to prior findings that normal sleep-wake cycles
304 require the activity of both proteins in neurons (Pfeiffenberger and Allada, 2012; Stavropoulos and
305 Young, 2011). The negative regulation of Inc by Cul3 in neurons is characteristic of autocatalytic
306 degradation exhibited by Cul3 adaptors (Djagaeva and Doronkin, 2009; Geyer et al., 2003; Hudson
307 and Cooley, 2010; Pintard et al., 2003; Wee et al., 2005; Zhang et al., 2005), providing further
308 support for the function of Inc as a Cul3 adaptor in cells through which Inc impacts sleep.

309 Our data and prior studies (Balasco et al., 2014; Dementieva et al., 2009; Ji et al., 2015)
310 suggest that Inc forms an obligate homopentamer in which neighboring Inc subunits interact
311 cooperatively. Consistent with a pentameric structure for Inc, a triple mutation altering opposite
312 sides of Inc and thus its interactions with both neighboring subunits severely compromised Inc
313 multimerization. Inc multimerization is furthermore required for efficient Cul3 binding, suggesting
314 that Cul3 binds cooperatively to the BTB domains of neighboring Inc subunits. Such a mechanism

315 is consistent with the consequences of mutating conserved phenylalanine residues (F47 and F105)
316 near this interface, which impair Cul3 binding and Inc function in vivo. It is perhaps surprising
317 that Inc mutants that impair Cul3 interactions do not elicit dominant negative phenotypes when
318 overexpressed, although we note that these mutants retain some ability to bind Cul3. Similarly, Inc
319 overexpression might be expected to sequester substrates but does not alter sleep (Li et al., 2017;
320 Stavropoulos and Young, 2011). We speculate that robust Inc homomultimerization may buffer
321 Cul3-Inc complexes against perturbations in Inc abundance and contribute, along with additional
322 mechanisms that regulate Inc activity, to the permissive influence that Inc exerts on sleep.

323 Our functional analysis of the Inc C-terminus provides insight into the mechanism by
324 which Inc is likely to bind substrates and orient them for ubiquitination in Cul3 complexes. The
325 Inc C-terminus is dispensable for Cul3 binding and Inc multimerization, yet is absolutely essential
326 for Inc function in vivo, implicating it as a substrate recruitment domain. We furthermore
327 identified a conserved, surface-exposed arginine residue (R135) within the Inc C-terminus
328 required for Inc activity in vivo. Mutation of this residue is behaviorally indistinguishable from
329 deleting the Inc C-terminus and does not alter Inc stability, suggesting that it does not disrupt the
330 structure of the C-terminal domain. While our results do not exclude the possibility that this residue
331 is essential for Inc trafficking or other mechanisms that might regulate Inc activity, the simplest
332 possibility suggested by its position on the lateral surface of the Inc C-terminus is that it contributes
333 directly to binding targets that impact sleep. A missense mutation of the same residue in the human
334 Inc ortholog KCTD17 (R145H) is associated with myoclonic dystonia (Mencacci et al., 2015),
335 suggesting a similar functional importance for substrate recruitment in Inc orthologs. The partial
336 functional impairment of Inc caused by removing C-terminal residues (Inc^{1-186}) is consistent with
337 the possibility that they contribute to substrate binding. These residues are not resolved in the

338 KCTD5 crystal structure (Dementieva et al., 2009), suggesting that they are flexible in the absence
339 of substrates and may become structured upon substrate binding. While a parsimonious model is
340 that Inc directly binds substrates, our findings do not rule out more complex models of substrate
341 recruitment that require co-adaptor proteins, analogous to the mechanism recently described for
342 KLHL12, a BTB-Kelch family adaptor (McGourty et al., 2016). Further studies are required to
343 elucidate Inc substrates and distinguish among these models.

344 Our recent findings revealed that orthologs of Inc can substitute for Inc in flies and
345 restore sleep to *inc* mutants, suggesting that the functions and targets of Inc and its orthologs are
346 evolutionarily conserved (Li et al., 2017). Our present studies provide evidence for the function
347 of Inc as a Cul3 adaptor in vivo and the foundation for identifying Inc substrates. While
348 substrates for Inc orthologs have been recently described in cultured cells (Brockmann et al.,
349 2017; Kasahara et al., 2014; Kim et al., 2017), whether these targets or other proteins mediate the
350 impact of Cul3 and Inc on sleep remains unknown. Elucidating Inc substrates and the
351 downstream pathways will advance our understanding of how protein ubiquitination pathways
352 contribute to the regulation of nervous system function and mechanisms underlying behavior.
353

354 **Acknowledgements**

355 We thank Zachary Zuchowski for assistance in constructing plasmids. This work was
356 supported by an International Student Research Fellowship from the Howard Hughes Medical
357 Institute (HHMI) to Q.L., and by grants from the National Institutes of Health (NS111304), the
358 Mathers Foundation, Whitehall Foundation grant 2013-05-78, fellowships from the Alfred P.
359 Sloan and Leon Levy Foundations, a NARSAD Young Investigator Award from the Brain and
360 Behavior Foundation, the J. Christian Gillin, M.D. Research Award from the Sleep Research
361 Society Foundation, and a Career Scientist Award from the Irma T. Hirschl/Weill-Caulier Trust
362 to N.S.

363

364

365 **Methods**

366 **Plasmids and molecular cloning**

367 Vectors for expression in S2 cells were as follows:

368 pAc5.1–Inc-HA (pNS277) encodes Inc fused to a C-terminal 1×HA epitope

369 (GSYPYDVPDYA) and was generated by ligating EcoRI-XhoI digested pAc5.1-v5-HisA

370 backbone and an EcoRI-XhoI Inc-HA fragment from pNS273 (as described below).

371 pAc5.1–3×Myc-Inc (pNS351) encodes an N-terminal 3×Myc epitope

372 (MEQKLISEEDLGSEQKLISEEDLGSEQKLISEEDLAS) fused to Inc as previously described

373 (Stavropoulos and Young, 2011).

374 pAc5.1–3×Myc-Inc$^{22-211}$ (pNS370) was generated by ligating NheI-XhoI digested

375 pNS309 (Stavropoulos and Young, 2011) and the NheI-XhoI fragment liberated from the PCR

376 amplification product of pNS351 template and primers oNS285 and oNS315.

377 pAc5.1–3×Myc-Inc$^{31-211}$ (pNS371) was generated similarly to pNS370, substituting

378 primers oNS285 and oNS316.

379 pAc5.1–3×Myc-Inc$^{124-211}$ (pNS372) was generated similarly to pNS370, substituting

380 primers oNS285 and oNS317.

381 pAc5.1–3×Myc-Inc$^{1-123}$ (pNS374) was generated similarly to pNS370, substituting

382 primers oNS277 and oNS319.

383 pAc5.1–3×Myc-Inc$^{1-156}$ (pNS375) was generated similarly to pNS370, substituting

384 primers oNS277 and oNS320.

385 pAc5.1–3×Myc-Inc$^{1-186}$ (pNS376) was generated similarly to pNS370, substituting

386 primers oNS277 and oNS321.

387 pAc5.1–3×HA-Inc (pNS402) encodes an N-terminal 3×HA epitope
388 (MYPYDVPDYAGSYPYDVPDYAGSYPYDVPDYAAS) fused to Inc and was generated by
389 ligating NheI-XhoI digested pNS310 (Stavropoulos and Young, 2011) and a NheI-XhoI *inc*
390 fragment liberated from pNS351.
391 pAc5.1–3×FLAG-Cul3 (pNS403) encodes an N-terminal 3×FLAG epitope
392 (MDYKDDDDKGSDYKDDDDKGSDYKDDDDKAS) fused to *Drosophila* Cul3 and was
393 generated by ligating NheI-NotI digested pNS311 and a NheI-NotI Cul3 fragment liberated from
394 pNS314 (Stavropoulos and Young, 2011). pNS311 contains an N-terminal 3×FLAG tag and was
395 generated from pNS298, a derivative of pAc5.1/V5-HisA that contains a C-terminal 3×FLAG
396 tag. To construct pNS298, oligonucleotides oNS234 and oNS235 were phosphorylated,
397 annealed, and cloned into XhoI-XbaI digested pAc5.1/V5-HisA. To construct pNS311, EcoRI-
398 NotI digested pAc5.1/V5-HisA was ligated to the EcoRI-NotI fragment liberated from the PCR
399 amplification product of pNS298 template and primers oNS240 and oNS241.
400 pAc5.1–3×FLAG-Inc (pNS408) encodes an N-terminal 3×FLAG epitope
401 (MDYKDDDDKGSDYKDDDDKGSDYKDDDDKAS) fused to Inc and was generated by
402 ligating NheI-NotI digested pNS311 and a NheI-XhoI *inc* fragment liberated from pNS351.
403 pAc5.1–3×HA-Inc^{F47A} (pNS409) encodes an N-terminal 3×HA epitope
404 (MYPYDVPDYAGSYPYDVPDYAGSYPYDVPDYAAS) fused to Inc^{F47A} and was generated
405 by ligating NheI-XhoI digested pNS310 and an NheI-XhoI Inc^{F47A} fragment. The NheI-XhoI
406 Inc^{F47A} fragment was liberated from the fusion PCR amplification product of primers oNS683
407 and oNS684 and an equimolar mix of overlapping 5' and 3' Inc^{F47A} fragments as template. The
408 5' and 3' fragments were generated by PCR amplification of pNS408 template with primers
409 oNS683/oNS695 and oNS684/oNS694, respectively.

410 pAc5.1–3×HA-Inc^{R50E} (pNS410) was generated similarly to pNS409, substituting
411 primers oNS683/oNS697 and oNS684/oNS696 for generating the 5' and 3' Inc^{R50E} fragments,
412 respectively.
413 pAc5.1–3×HA-Inc^{D57A} (pNS411) was generated similarly to pNS409, substituting
414 primers oNS683/oNS699 and oNS684/oNS698 for generating the 5' and 3' Inc^{D57A} fragments,
415 respectively.
416 pAc5.1–3×HA-Inc^{D61A} (pNS412) was generated similarly to pNS409, substituting
417 primers oNS683/oNS701 and oNS684/oNS700 for generating the 5' and 3' Inc^{D61A} fragments.,
418 respectively.
419 pAc5.1–3×HA-Inc^{E104K} (pNS413) was generated similarly to pNS409, substituting
420 primers oNS683/oNS703 and oNS684/oNS702 for generating the 5' and 3' Inc^{E104K} fragments,
421 respectively.
422 pAc5.1–3×HA-Inc^{D73A} (pNS430) was generated similarly to pNS409, substituting
423 primers oNS683/oNS686 and oNS684/oNS685 for generating the 5' and 3' Inc^{D73A} fragments,
424 respectively.
425 pAc5.1–3×HA-Inc^{N82A} (pNS431) was generated similarly to pNS409, substituting
426 primers oNS683/oNS686 and oNS684/oNS685 for generating the 5' and 3' Inc^{N82A} fragments,
427 respectively.
428 pAc5.1–3×HA-Inc^{K88D} (pNS432) was generated similarly to pNS409, substituting
429 primers oNS683/oNS688 and oNS684/oNS687 for generating the 5' and 3' Inc^{K88D} fragments,
430 respectively.
431

432 pAc5.1–3×HA-Inc^{E101K} (pNS433) was generated similarly to pNS409, substituting
433 primers oNS683/oNS688 and oNS684/oNS687 for generating the 5' and 3' Inc^{E101K} fragments,
434 respectively.
435 pAc5.1–3×HA-Inc^{T36A} (pNS434) was generated similarly to pNS409, substituting
436 primers oNS683/oNS693 and oNS684/oNS689 for generating the 5' and 3' Inc^{T36A} fragments,
437 respectively.
438 pAc5.1–3×HA-Inc^{D71A} (pNS435) was generated similarly to pNS409, substituting
439 primers oNS683/oNS693 and oNS684/oNS689 for generating the 5' and 3' Inc^{D71A} fragments,
440 respectively.
441 pAc5.1–3×HA-Inc^{R85E} (pNS436) was generated similarly to pNS409, substituting
442 primers oNS683/oNS692 and oNS684/oNS691 for generating the 5' and 3' Inc^{R85E} fragments,
443 respectively.
444 pAc5.1–3×HA-Inc$^{D73A/N82A}$ (pNS414) was generated similarly to pNS409, substituting
445 pNS430 template and primers oNS683/oNS686 for generating the 5' Inc$^{D73A/N82A}$ fragment; and
446 pNS431 template and primers oNS684/oNS685 for generating the 3' Inc$^{D73A/N82A}$ fragment.
447 pAc5.1–3×HA-Inc$^{K88D/E101K}$ (pNS415) was generated similarly to pNS409, substituting
448 pNS432 template and primers oNS683/oNS688 for generating the 5' Inc$^{K88D/E101K}$ fragment; and
449 pNS433 template and primers oNS684/oNS687 for generating the 3' Inc$^{K88D/E101K}$ fragment.
450 pAc5.1–3×HA-Inc$^{T36A/D71A}$ (pNS416) was generated similarly to pNS409, substituting
451 pNS434 template and primers oNS683/oNS693 for generating the 5' Inc$^{T36A/D71A}$ fragment; and
452 pNS435 template and primers oNS684/oNS689 for generating the 3' Inc$^{T36A/D71A}$ fragment.

453 pAc5.1–3×HA-Inc$^{D71A/R85E}$ (pNS417) was generated similarly to pNS409, substituting
454 pNS435 template and primers oNS683/oNS692 for generating the 5' Inc$^{D71A/R85E}$ fragment; and
455 pNS436 template and primers oNS684/oNS691 for generating the 3' Inc $^{D71A/R85E}$ fragment.
456 pAc5.1–3×HA-Inc$^{T36A/D71A/R85E}$ (pNS418) was generated by ligating EcoRV-XhoI
457 digested pNS434 backbone and an EcoRV-XhoI 3×HA-Inc$^{D71A/R85E}$ fragment from pNS417.
458 pAc5.1–3×HA-Inc^{F105A} (pNS419) was generated similarly to pNS409, substituting
459 primers oNS683/oNS1123 and oNS684/oNS1122 for generating the 5' and 3' Inc^{F105A}
460 fragments, respectively.
461 pAc5.1–3×HA-Inc^{Y106F} (pNS420) was generated similarly to pNS409, substituting
462 primers oNS683/oNS1146 and oNS684/oNS1145 for generating the 5' and 3' Inc^{Y106F}
463 fragments, respectively.
464 pAc5.1–3×HA-Inc^{N107A} (pNS421) was generated similarly to pNS409, substituting
465 primers oNS683/oNS1125 and oNS684/oNS1124 for generating the 5' and 3' Inc^{N107A}
466 fragments, respectively.
467 pAc5.1–3×HA-Inc$^{F47A/F105A}$ (pNS422) was generated similarly to pNS409, substituting
468 pNS409 template, primers oNS683/oNS1123, and oNS684/oNS1122 for generating the 5' and 3'
469 Inc$^{F47A/F105A}$ fragments, respectively.
470 pAc5.1–3×HA-Inc^{R135H} (pNS426) was generated by ligating HindIII-XhoI digested
471 pNS402 backbone and a HindIII-XhoI Inc^{R135H} fragment from pNS428 (as described below).
472 pAc5.1–3×HA-Inc^{AAA} (pNS427) was generated similarly to pNS426, substituting a
473 HindIII-XhoI Inc^{AAA} fragment from pNS429 (as described below).
474
475 Vectors for *Drosophila* transgenesis were as follows:

476 pUASTattB–Myc-Inc (pNS346) encodes an N-terminal Myc epitope
477 (MEQKLISEEDLAS) fused to Inc, as previously described (Li et al., 2017).
478 pUASTattB–Myc-Inc^{R135H} (pNS428) was generated by ligating a HindIII-XhoI digested
479 pNS346 backbone and a HindIII-XhoI Inc^{R135H} fragment. The Inc^{R135H} fragment was liberated
480 from the fusion PCR amplification product of primers oNS1126 and oNS1127 and an equimolar
481 mix of overlapping 5' and 3' Inc^{R135H} fragments as template. The 5' and 3' fragments were
482 generated by PCR amplification of pNS346 template with primers oNS1126/oNS1555 and
483 oNS1127/oNS1554, respectively.
484 pUASTattB–Myc-Inc^{AAA} (pNS429) was generated similarly as pNS428, substituting a
485 HindIII-XhoI Inc^{AAA} fragment. The Inc^{AAA} fragment was generated similarly as Inc^{R135H},
486 substituting primers oNS1126/oNS1557 and oNS1127/oNS1556 for generating the 5' and 3'
487 Inc^{AAA} fragments, respectively.
488 pUAST–Inc-HA (pNS273) encodes Inc fused to a C-terminal HA epitope
489 (GSYPYDVPDYA) and was generated by three piece ligation of pUAST BglII-XhoI, a BglII-
490 EcoRI *inc* fragment liberated from pNS272 (Stavropoulos and Young, 2011), and an EcoRI-
491 XhoI HA fragment generated by phosphorylating and annealing oligonucleotides oNS191 and
492 oNS192.
493 pUASTattB–3×FLAG-Inc (pNS404) encodes an N-terminal 3×FLAG epitope
494 (MDYKDDDDKGSDYKDDDDKGSDYKDDDDKAS) fused to Inc and was generated by three
495 piece ligation of EcoRI-XhoI digested pUASTattB, an EcoRI-NheI 3×FLAG fragment liberated
496 from the PCR amplification product of pNS311 template and primers ACF and oNS241, and a
497 NheI-XhoI *inc* fragment liberated from pNS351.

498 pUASTattB–3×FLAG- Inc^{1-186} (pNS405) was generated similar to pNS404, substituting a
499 NheI-XhoI Inc fragment prepared as for pNS376.
500 pUASTattB–3×FLAG-Inc^{1-156} (pNS406) was generated similar to pNS404, substituting a
501 NheI-XhoI Inc fragment prepared as for pNS375.
502 pUASTattB–3×FLAG- Inc^{1-123} (pNS407) was generated similar to pNS404, substituting a
503 NheI-XhoI Inc fragment prepared as for pNS374.
504 pUASTattB–3×FLAG-Inc^{F47A} (pNS423) was generated similar to pNS404, substituting a
505 NheI-XhoI Inc fragment prepared as for pNS409.
506 pUASTattB–3×FLAG-Inc^{F105A} (pNS424) was generated similar to pNS404, substituting a
507 NheI-XhoI Inc fragment prepared as for pNS419.
508 pUASTattB–3×FLAG-$Inc^{F47A/F105A}$ (pNS425) was generated similar to pNS404,
509 substituting a NheI-XhoI Inc fragment prepared as for pNS422.
510
511 **Oligonucleotides**
512 Oligonucleotides used in this work, listed 5' to 3', are as follows:
513 oNS98 ACTGGGATCCTGGGAGCACGAGCAGCAAAGGAG
514 oNS184 CCAGCCATCCGACAGCGTTGAGATC
515 oNS191
516 AATTTTGGGAATTGGATCCTACCCCTACGATGTGCCCGATTACGCCTAAC
517
518 oNS192
519 TCGAGTTAGGCGTAATCGGGCACATCGTAGGGGTAGGATCCAATTCCCAA
520

521 oNS234

522 TCGAGGCTAGCGACTACAAGGATGATGACGATAAGGGCTCCGATTACAAGGA

523 CGACGATGATAAGGGATCCGATTACAAGGATGATGACGACAAGTGAT

524 oNS235

525 CTAGATCACTTGTCGTCATCATCCTTGTAATCGGATCCCTTATCATCGTCGTCC

526 TTGTAATCGGAGCCCTTATCGTCATCATCCTTGTAGTCGCTAGCC

527 oNS240

528 ACTGGAATTCCGCGGCAACATGGACTACAAGGATGATGACGATAAGGGC

529 oNS241

530 ACTGGCGGCCGCTCCTAGGGTGCTAGCCTTGTCGTCATCATCCTTGTAATCGG

531 AT

532 oNS277 ACGTGCTAGCATGAGCACGGTGTTCATAAACTCGC

533 oNS283 GATCTCAACATGGAGCAGAAGCTGATCAGCGAGGAGGATCTGG

534 oNS284 CTAGCCAGATCCTCCTCGCTGATCAGCTTCTGCTCCATGTTGA

535 oNS285 ACGTGCTAGCTCGAGGGGTTGTGTGTGAATATATAGCGCGA

536 oNS315 ACGTGCTAGCCAGTGGGTCAAGCTGAACGTAG

537 oNS316 ACGTGCTAGCACCTACTTCCTCACCACAAAGACG

538 oNS317 ACGTGCTAGCCAGCGACCCCAAACGGACAA

539 oNS319 ACGTCTCGAGTTAATCCCTGTGCAGGATGCACTC

540 oNS320 ACGTCTCGAGTTACCTCCAGCCATCCGACAG

541 oNS321 ACGTCTCGAGTTATGTGCCACACTCTTTGGATACCA

542 oNS337 TTTTTTTTTTTTTTTTTTTTTTTVN

543 oNS683 ACGTGCTAGCATGAGCACGGTGTTCATAAACTCGC

544	oNS684	ACGTCTCGAGGGGTTGTGTGTGAATATATAGCGCGA
545	oNS685	CCTGATCGACAGAGCCCCCAAATACTTTGC
546	oNS686	GGCGCAGGTAGGCGAGCACGGGTGCAAA
547	oNS687	TGCGCCACGGCGACCTTGTGCTCGAT
548	oNS688	TAGAACTCAGCCTCCTTCAGGACGCCTTC
549	oNS689	CTACTTCCTCACCGCCAAGACGACGCTC
550	oNS691	GCCTACCTGATCGCCAGAGACCCCAAA
551	oNS692	CAAGCTTGCCGTGTTCCAGGTAATTGAGC
552	oNS693	TTTGGGGTCTCTGGCGATCAGGTAGGC
553	oNS694	GACCCAAATTCGGCCCTCTCCCGTCTG
554	oNS695	CAGACGGGAGAGGGCCGAATTTGGGTC
555	oNS696	TCGTTCCTCTCCGAACTGATTCAGGAGG
556	oNS697	CCTCCTGAATCAGTTCGGAGAGGAACGA
557	oNS698	CAGGAGGACTGCGCCTTGATATCAGATCG
558	oNS699	CGATCTGATATCAAGGCGCAGTCCTCCTG
559	oNS700	CGACTTGATATCAGCCCGGGACGAGAC
560	oNS701	GTCTCGTCCCGGGCTGATATCAAGTCG
561	oNS702	CCTGGAGGAGGCTAAGTTCTACAACGTGAC
562	oNS703	GTCACGTTGTAGAACTTAGCCTCCTCCAGG
563	oNS810	ATGCTACTTTTGTCGCCCATCGC
564	oNS811	CTGGGTTATCCTTGGTTTATCCTGGCCT
565	oNS1122	GGAGGCTGAGGCCTACAACGTGAC
566	oNS1123	GTCACGTTGTAGGCCTCAGCCTCC

567 oNS1124 GCTGAGTTCTACGCCGTGACGCAGC

568 oNS1125 GCTGCGTCACGGCGTAGAACTCAGC

569 oNS1126 CAACTGCAACTACTGAAARCRGCCAAGAAG

570 oNS1127 GGTAGTTTGTCCAATTATGTCACACCACAGAAG

571 oNS1145 GAGGCTGAGTTCTTCAACGTGACGCAGC

572 oNS1146 GCTGCGTCACGTTGAAGAACTCAGCCTC

573 oNS1554 AAGCGCGTTTATCATGTGCTGCAGTGC

574 oNS1555 GCACTGCAGCACATGATAAACGCGCTT

575 oNS1556

576 ATCAGCATGCAGTACACGGCCGCCGCGCCCTTCGAAAACAATGAGTTCCTG

577 oNS1557 ATTGTTTTCGAAGGGCGCGGCGGCCGTGTACTGCATGCTGATCAGCT

578 ACF GACACAAAGCCGCTCCATCAG

579 attP2-5' CACTGGCACTAGAACAAAAGCTTTGGCG

580 RPS3A CGAACCTTCCGATTTCCAAGAAACGC

581 RPS3B ACGACGGACGGCCAGTCCTCC

582

583 **Cell culture and biochemistry**

584 S2 cells were cultured in S2 media containing 10% FBS, penicillin, and streptomycin,

585 and were transfected with Effectene (Qiagen) as described previously (Stavropoulos and Young,

586 2011). Transfections were performed in 6 well plates for ~24 hr, after which liposome-

587 containing media was replaced with fresh culture media. 400 ng of total DNA was used for each

588 transfection. For transfections involving two plasmids, an equal amount of each was used. Empty

589 vector lacking insert was used to equalize DNA amounts as indicated in Figures . Cells were

590 harvested 36-48 hr after transfections were initiated, washed twice in PBS, and lysed in ice-cold
591 NP40 lysis buffer (50 mM Tris pH 7.6, 150mM NaCl, 0.5% NP40) containing protease
592 inhibitors. Protein extracts were quantitated in duplicate (BioRad, 5000111).
593 For co-immunoprecipitations of truncated Inc proteins from S2 cells, 700-1000 µg total
594 protein was incubated overnight at 4°C with 1:100 anti-FLAG (Sigma, F1804) or anti-Myc
595 (Sigma, C3956) antibody. Complexes were precipitated by incubation with Gammabind G
596 sepharose beads (Life Technologies, 10-1243) for 1 hr at 4°C on a nutator, washed 4×5 min at
597 4°C with lysis buffer, and denatured in SDS sample buffer, separated on Tris SDS-PAGE gels,
598 and transferred to nitrocellulose. For co-immunoprecipitations of Inc point mutant proteins from
599 S2 cells, 450-1000 µg of total protein was immunoprecipitated overnight with 20 µl (50% slurry)
600 of anti-FLAG (Sigma, F2426) affinity gel at 4°C on a nutator. Samples were then washed 4×5
601 min at 4°C with lysis buffer, denatured in SDS sample buffer, separated on Tris SDS-PAGE
602 gels, and transferred to nitrocellulose. Membranes were blocked for 1-1.5 hr at room temperature
603 in LI-COR Odyssey buffer (LI-COR, 927-40000). Membranes were subsequently incubated in
604 blocking buffer containing 0.1% Tween 20 and the appropriate primary antibodies for 1-2 hr at
605 room temperature or 4°C overnight: rabbit anti-Myc (1:2,000, Sigma, C3956), mouse anti-FLAG
606 (1:2,000, Sigma, F1804), rat anti-HA (1:2,000, Roche, 11867431001), and rabbit anti-HA
607 (1:2,000, Bethyl Laboratories, A190-208A). After washing 4×5 min in a solution containing 150
608 mM NaCl, 10mM Tris pH 7.6, and 0.1% Tween 20 (TBST), membranes were incubated in the
609 dark for 30-60 min at room temperature with appropriate secondary antibodies, all diluted
610 1:15,000 or 1:30,000 in blocking buffer containing 0.1% Tween 20 and 0.01% SDS: Alexa 680
611 donkey anti-rabbit (Life Technologies, A10043), Alexa 680 donkey anti-mouse (Life
612 Technologies, A10038), Alexa 790 anti-mouse (Life Technologies, A11371), Alexa 790 anti-rat

613 (Jackson ImmunoResearch, 712-655-153). Membranes were then washed 4×5 min in TBST, 1×5
614 min in TBS, and imaged on a Li-Cor Odyssey CLx instrument.
615 Fly protein extracts were prepared from whole animals or from sieved heads by manual
616 pestle homogenization in ice-cold NP40 lysis buffer supplemented with protease inhibitors. For
617 co-immunoprecipitation from fly head protein extracts, complexes were immunoprecipitated
618 with 30 µl (50% slurry) of anti-Myc (Sigma, E6654) affinity gel for 1.5 hr at 4°C on a nutator.
619 Samples were then washed 4×5 min at 4°C with lysis buffer, denatured in SDS sample buffer,
620 separated on Tris SDS-PAGE gels and blotted as described above. Primary antibodies were
621 rabbit anti-Myc (1:2,000, Sigma, C3956), mouse anti-FLAG (1:2,000, Sigma, F1804), and rat
622 anti-HA (1:2,000, Roche, 11867431001). Secondary antibodies were Alexa 680 donkey anti-rat
623 (Jackson ImmunoResearch, 712-625-1533), Alexa 680 donkey anti-mouse (Life Technologies,
624 A10038), Alexa 790 anti-rabbit (Life Technologies, A11374). For assessing in vivo expression
625 of Inc proteins, 30 µg was separated on Tris-SDS-PAGE gels and blotted as described above.
626 Primary antibodies were rabbit anti-Myc (1:2,000, Sigma, C3956), mouse anti-FLAG (1:2,000,
627 Sigma, F1804), mouse anti-tubulin (1:10,000, DSHB, 12G10), and rabbit anti-tubulin (1:60,000,
628 VWR, 89364-004). Secondary antibodies were Alexa 680 anti-mouse (Life Technologies,
629 A10038) and Alexa 790 anti-rabbit (Life Technologies, A11374).
630
631 **qRT-PCR**
632 Total RNA was isolated using TRIZOL (Life Technologies, 15596-026). 5 µg of RNA
633 was reverse transcribed with a poly-T primer (oNS337) and SuperScript II reverse transcriptase.
634 qPCR was performed using SYBR Green Supermix (Bio-Rad, 1725272) and the following

635 primers: oNS98 and oNS184 (*inc*); oNS810 and oNS811 (*Cul3*); RPS3A and RPS3B (*rps3*). All
636 real-time PCR reactions were performed using a BioRad DNA Engine Opticon 2 System.
637
638 **Fly stocks and transgenes**
639 *elav^{c155}-Gal4* (Lin and Goodman, 1994), *inc^{1}* (Stavropoulos and Young, 2011), *inc-Gal4*
640 (Stavropoulos and Young, 2011), *inc^{1} inc-Gal4* (Li et al., 2017), *attP2: UAS-Myc-Inc* (Li et al.,
641 2017), *attP2: UAS-3×FLAG-Inc* (Li et al., 2017), and *UAS-3×FLAG-3×HA-Cul3* (Hudson and
642 Cooley, 2010) are previously described. *UAS-Cul3-RNAi* is 11861R-2 obtained from the NIG-
643 Fly stock center. Transgenic flies generated in this study using pUASTattB-based vectors were
644 integrated at *attP2* (Groth et al., 2004) with phiC31 recombinase (BestGene); integration was
645 verified by PCR using primer attP2-5' paired with oNS277. All transgenes were backcrossed six
646 to eight generations to Bloomington stock 5905, an isogenic *w^{1118}* stock described elsewhere as
647 iso31 (Ryder et al., 2004).
648
649 **Sleep analysis**
650 Crosses were set with five virgin females and three males on cornmeal, agar, and
651 molasses food. One to four day old male flies eclosing from LD-entrained cultures raised at 25°C
652 were loaded in glass tubes containing cornmeal, agar, and molasses food. Animals were
653 monitored for 5-7 days at 25°C in LD cycles using DAM2 monitors (Trikinetics). The first 36-48
654 hours of data were discarded and an integral number of days of data (3-5) were analyzed using
655 custom Matlab code. Locomotor data were collected in 1 min bins. Sleep was defined by
656 locomotor inactivity for 5 min or more; all minutes within inactive periods exceeding 5 min were
657 assigned as sleep. This definition classifies more sleep than the definition used in our prior

658 studies (Li et al., 2017; Li and Stavropoulos, 2016; Stavropoulos and Young, 2011), in which
659 sleep is scored as beginning on the fifth minute of locomotor inactivity and the preceding four
660 minutes are classified as quiet wakefulness. Dead animals were excluded from analysis by a
661 combination of automated filtering and visual inspection of locomotor traces.
662
663 **Statistics**
664 One-way ANOVA and Tukey post-hoc tests were used for comparisons of total sleep,
665 daytime sleep, nighttime sleep, and sleep bout number. Nonparametric Kruskal-Wallis tests and
666 Dunn's post hoc tests were used for comparisons of sleep bout length. Unpaired two-sided
667 Student's t-tests were used for comparisons of *inc* mRNA levels in vivo.
668
669 **Sequence alignments**
670 Alignments were performed with Clustal Omega 2.1 and BOXSHADE. GenBank
671 accession numbers for proteins in Figure S1A are: Inc, NP_001284787; KCTD2, NP_056168;
672 KCTD5, NP_061865; KCTD17.3, NP_001269614; KCTD17.4, NP_001269615.
673

674 **Figure Legends**

675

676 **Figure 1. The Inc BTB domain mediates Inc-Cul3 and Inc-Inc associations**

677 **A)** Schematic of N- and C-terminally truncated Inc proteins. CTD, C-terminal domain. **B and C)**
678 Co-immunoprecipitation of 3×Myc-tagged Inc or Inc truncation proteins with 3×FLAG-Cul3 (**B)**
679 or Inc-HA **(C)** from transiently transfected S2 cells. LC, immunoglobulin light chain.

680

681 **Figure 2. Identification of Inc BTB domain point mutants that specifically weaken Inc-Cul3**
682 **associations**

683 **A-D)** Co-immunoprecipitation analysis of 3×HA-tagged Inc or Inc point mutants and 3×FLAG-
684 Cul3 **(A and C)** or 3×FLAG-Inc **(B and D)** from transiently transfected S2 cells.

685

686 **Figure 3. Inc-Cul3 binding is required for Inc activity in vivo**

687 Biochemical and behavioral analysis of *inc*^{1} *inc-Gal4* animals expressing 3×FLAG-tagged Inc or
688 Inc point mutants that weaken Cul3 associations. **A)** Immunoblot analysis of whole animal lysates.
689 **B)** Total sleep duration. Mean ± SEM is shown. n = 16-58; *$p < 0.01$ for comparison to *inc*^{1} *inc-*
690 *Gal4* animals and not significantly different from wild-type controls; ‡$p < 0.01$ for comparisons to
691 *inc*^{1} *inc-Gal4* animals and wild-type controls. **C)** Population average sleep traces summed hourly
692 for indicated genotypes. n = 41-58. For all panels, animals are heterozygous for UAS transgenes.

693

694 **Figure 4. The conserved Inc C-terminus is essential for Inc activity in vivo**

695 Biochemical and behavioral analysis of *inc*^{1} *inc-Gal4* animals expressing 3×FLAG-tagged Inc or
696 C-terminally truncated Inc proteins. **A)** Immunoblot analysis of whole animal lysates. **B)** Total

697 sleep duration. Mean ± SEM is shown. n = 27-30; *p < 0.01 for comparison to *inc*[1] *inc-Gal4*
698 animals and not significantly different from wild-type controls. **C)** Population average sleep traces
699 summed hourly for indicated genotypes. n = 27-30. For all panels, animals are heterozygous for
700 UAS transgenes.
701
702 **Figure 5. Inc C-terminal point mutants do not alter Inc-Cul3 and Inc-Inc associations**
703 Co-immunoprecipitation analysis of 3×HA-tagged Inc or Inc point mutants and 3×FLAG-Cul3 or
704 3×FLAG-Inc from transiently transfected S2 cells.
705
706 **Figure 6. The conserved Inc C-terminal arginine is vital for Inc activity in vivo**
707 Biochemical and behavioral analysis of *inc*[1] *inc-Gal4* animals expressing 3×Myc-tagged Inc or
708 Inc point mutants. **A)** Immunoblot analysis of whole animal lysates. **B)** Total sleep duration. Mean
709 ± SEM is shown. n = 24-46; *p < 0.01 for comparison to *inc*[1] *inc-Gal4* animals and not
710 significantly different from wild-type controls. **C)** Population average sleep traces summed hourly
711 for indicated genotypes. n = 24-46. For all panels, animals are heterozygous for UAS transgenes.
712
713 **Figure 7. Inc exhibits key properties of a Cul3 adaptor in neurons in vivo**
714 Co-immunoprecipitation analysis of 3×Myc-tagged Inc and 3×FLAG-3×HA-Cul3 **(A)** or 3×HA-
715 Inc **(B)** from head lysates prepared from indicated genotypes. **C)** Western blots of head lysates
716 prepared from indicated genotypes. **D)** qRT-PCR analysis of *inc* mRNA levels of indicated
717 genotypes. Mean ± SEM is shown. *p < 0.05; ns, not significant (p>0.05).
718

719 **Table 1. Summary of co-immunoprecipitation analysis of Inc point mutants designed to**

720 **weaken Inc-Cul3 interaction from transfected S2 cells**

721

722

723 **Table 2. Summary of co-immunoprecipitation analysis of Inc point mutants designed to**

724 **weaken Inc-Inc interaction from transfected S2 cells**

725

726

727 **Supplementary Figure 1. Sequence and crystal structure analysis of Inc and human Inc**
728 **orthologs**
729 **(A)** Alignment of Inc and its human orthologs. Identical and similar residues are shaded in black
730 and gray, respectively. Locations of Inc truncations are indicated by arrowheads. Inc point mutants
731 are indicated by closed circles. **(B)** Crystal structure of the BTB domains of adjacent subunits of
732 human KCTD5. Residues that do not impair Inc-Cul3 association when mutated are highlighted
733 in cyan. Mutations that weaken Inc-Cul3 associations (F47A and F105A) are highlighted in blue.
734 **(C)** Crystal structure of the BTB domains of adjacent subunits of human KCTD5. Residues
735 mutated to impair Inc-Inc association are indicated. The T36A/D71A/R85E triple mutation
736 weakens Inc homomultimerization and decreases Inc stability. **(D)** Crystal structure of human
737 KCTD5. Inc C-terminal point mutants are indicated.
738
739 **Supplementary Figure 2. Neuronal expression of Inc BTB-domain point mutants does not**
740 **perturb sleep**
741 **(A)** Biochemical analysis of *inc-Gal4* animals expressing 3×FLAG-tagged Inc or Inc point mutants.
742 **(B)** Behavioral analysis of *elav*^{c155}*-Gal4* animals expressing 3×FLAG-tagged Inc or Inc point
743 mutants. Mean ± SEM is shown. n = 5-24; ns, not significant ($p>0.05$) compared to *elav*^{c155}*-Gal4*
744 control. For all panels, animals are heterozygous for UAS transgenes.
745
746 **Supplementary Figure 3. Additional sleep parameters for animals expressing Inc and Inc**
747 **BTB domain point mutants**
748 **(A-D)** Sleep parameters for *inc*^{1} *inc-Gal4* animals expressing 3×FLAG-tagged Inc or Inc point
749 mutants. Mean ± SEM is shown. n = 16-58 as in Fig 3B; *$p < 0.01$ for comparison to *inc*^{1} *inc-Gal4*

750 animals and not significantly different from wild-type controls; ‡p < 0.01 for comparisons to *inc*^{1}
751 *inc-Gal4* animals and wild-type controls. **A)** Nighttime sleep. **B)** Daytime sleep. **C)** Sleep bout
752 duration. **D)** Sleep bout number. For all panels, animals are heterozygous for UAS transgenes.
753
754 **Supplementary Figure 4. Neuronal expression of Inc C-terminal truncations does not alter**
755 **sleep**
756 Behavioral analysis of *elav*^{c155}*-Gal4* animals expressing 3×FLAG-tagged Inc or C-terminally
757 truncated Inc proteins. Mean ± SEM is shown. n = 23-54; ns, not significant (p>0.05) compared
758 to *elav*^{c155}*-Gal4* control. For all panels, animals are heterozygous for UAS transgenes.
759
760 **Supplementary Figure 5. Additional sleep parameters for animals expressing Inc C-terminal**
761 **truncations**
762 **(A-D)** Sleep parameters for *inc*^{1} *inc-Gal4* animals expressing 3×FLAG-tagged Inc or C-terminally
763 truncated Inc proteins. Mean ± SEM is shown. n = 27-30 as in Fig 4B; *p < 0.01 for comparison
764 to *inc*^{1} *inc-Gal4* animals and not significantly different from wild-type controls; ‡p < 0.01 for
765 comparisons to *inc*^{1} *inc-Gal4* animals and wild-type controls. **A)** Nighttime sleep. **B)** Daytime
766 sleep. **C)** Sleep bout duration. **D)** Sleep bout number. For all panels, animals are heterozygous for
767 UAS transgenes.
768
769 **Supplementary Figure 6. Neuronal expression of Inc C-terminal point mutants does not**
770 **perturb sleep**

771 Behavioral analysis of *elav*^{c155}-*Gal4* animals expressing 3×Myc-tagged Inc or Inc point mutants.
772 Mean ± SEM is shown. n = 18-65; ns, not significant (p>0.05) compared to *elav*^{c155}-*Gal4* control.
773 For all panels, animals are heterozygous for UAS transgenes.
774
775 **Supplementary Figure 7. Additional sleep parameters for animals expressing Inc C-terminal**
776 **point mutants.**
777 **(A-D)** Sleep parameters for *inc*^{1} *inc-Gal4* animals expressing 3×Myc-tagged Inc or Inc point
778 mutants. Mean ± SEM is shown. n = 24-46 as in Fig 4B; *p < 0.01 for comparison to *inc*^{1} *inc-Gal4*
779 animals and not significantly different from wild-type controls; ‡p < 0.01 for comparisons to *inc*^{1}
780 *inc-Gal4* animals and wild-type controls. **A)** Nighttime sleep. **B)** Daytime sleep. **C)** Sleep bout
781 duration. **D)** Sleep bout number. For all panels, animals are heterozygous for UAS transgenes.
782
783
784
785
786
787
788
789
790
791
792
793

794 **References**

795

796 Afonso, D.J.S., Liu, D., Machado, D.R., Pan, H., Jepson, J.E.C., Rogulja, D., Koh, K., 2015.
797 TARANIS Functions with Cyclin A and Cdk1 in a Novel Arousal Center to Control Sleep in
798 Drosophila. Curr Biol 25, 1717–1726. doi:10.1016/j.cub.2015.05.037
799
800 Balasco, N., Pirone, L., Smaldone, G., Di Gaetano, S., Esposito, L., Pedone, E.M., Vitagliano,
801 L., 2014. Molecular recognition of Cullin3 by KCTDs: insights from experimental and
802 computational investigations. Biochim. Biophys. Acta 1844, 1289–1298.
803 doi:10.1016/j.bbapap.2014.04.006
804
805 Brockmann, M., Blomen, V.A., Nieuwenhuis, J., Stickel, E., Raaben, M., Bleijerveld, O.B.,
806 Altelaar, A.F.M., Jae, L.T., Brummelkamp, T.R., 2017. Genetic wiring maps of single-cell
807 protein states reveal an off-switch for GPCR signalling. Nature 546, 307–311.
808 doi:10.1038/nature22376
809
810 Butler, A., Wei, A.G., Baker, K., Salkoff, L., 1989. A family of putative potassium channel
811 genes in Drosophila. Science 243, 943–947. doi:10.1126/science.2493160
812
813 Canning, P., Cooper, C.D.O., Krojer, T., Murray, J.W., Pike, A.C.W., Chaikuad, A., Keates, T.,
814 Thangaratnarajah, C., Hojzan, V., Ayinampudi, V., Marsden, B.D., Gileadi, O., Knapp, S.,
815 Delft, von, F., Bullock, A.N., 2013. Structural basis for Cul3 protein assembly with the
816 BTB-Kelch family of E3 ubiquitin ligases. J Biol Chem 288, 7803–7814.
817 doi:10.1074/jbc.M112.437996
818
819 Chiu, C.N., Rihel, J., Lee, D.A., Singh, C., Mosser, E.A., Chen, S., Sapin, V., Pham, U., Engle,
820 J., Niles, B.J., Montz, C.J., Chakravarthy, S., Zimmerman, S., Salehi-Ashtiani, K., Vidal, M.,
821 Schier, A.F., Prober, D.A., 2016. A Zebrafish Genetic Screen Identifies Neuromedin U as a
822 Regulator of Sleep/Wake States. Neuron 89, 842–856. doi:10.1016/j.neuron.2016.01.007
823
824 Cirelli, C., Bushey, D., Hill, S., Huber, R., Kreber, R., Ganetzky, B., Tononi, G., 2005. Reduced
825 sleep in Drosophila Shaker mutants. Nature 434, 1087–1092. doi:10.1038/nature03486
826
827 Dementieva, I.S., Tereshko, V., McCrossan, Z.A., Solomaha, E., Araki, D., Xu, C., Grigorieff,
828 N., Goldstein, S.A.N., 2009. Pentameric assembly of potassium channel tetramerization
829 domain-containing protein 5. J Mol Biol 387, 175–191. doi:10.1016/j.jmb.2009.01.030
830
831 DiBello, P.R., Withers, D.A., Bayer, C.A., Fristrom, J.W., Guild, G.M., 1991. The Drosophila
832 Broad-Complex encodes a family of related proteins containing zinc fingers. Genetics 129,
833 385–397.
834
835 Djagaeva, I., Doronkin, S., 2009. COP9 limits dendritic branching via Cullin3-dependent
836 degradation of the actin-crosslinking BTB-domain protein Kelch. PLoS ONE 4, e7598.
837 doi:10.1371/journal.pone.0007598
838

839 Emanuele, M.J., Elia, A.E.H., Xu, Q., Thoma, C.R., Izhar, L., Leng, Y., Guo, A., Chen, Y.-N.,
840 Rush, J., Hsu, P.W.-C., Yen, H.-C.S., Elledge, S.J., 2011. Global identification of modular
841 cullin-RING ligase substrates. Cell 147, 459–474. doi:10.1016/j.cell.2011.09.019
842
843 Errington, W.J., Khan, M.Q., Bueler, S.A., Rubinstein, J.L., Chakrabartty, A., Privé, G.G., 2012.
844 Adaptor protein self-assembly drives the control of a cullin-RING ubiquitin ligase. Structure
845 20, 1141–1153. doi:10.1016/j.str.2012.04.009
846
847 Funato, H., Miyoshi, C., Fujiyama, T., Kanda, T., Sato, M., Wang, Z., Ma, J., Nakane, S.,
848 Tomita, J., Ikkyu, A., Kakizaki, M., Hotta-Hirashima, N., Kanno, S., Komiya, H., Asano, F.,
849 Honda, T., Kim, S.J., Harano, K., Muramoto, H., Yonezawa, T., Mizuno, S., Miyazaki, S.,
850 Connor, L., Kumar, V., Miura, I., Suzuki, T., Watanabe, A., Abe, M., Sugiyama, F.,
851 Takahashi, S., Sakimura, K., Hayashi, Y., Liu, Q., Kume, K., Wakana, S., Takahashi, J.S.,
852 Yanagisawa, M., 2016. Forward-genetics analysis of sleep in randomly mutagenized mice.
853 Nature 539, 378–383. doi:10.1038/nature20142
854
855 Furukawa, M., He, Y.J., Borchers, C., Xiong, Y., 2003. Targeting of protein ubiquitination by
856 BTB-Cullin 3-Roc1 ubiquitin ligases. Nat Cell Biol 5, 1001–1007. doi:10.1038/ncb1056
857
858 Geyer, R., Wee, S., Anderson, S., Yates, J., Wolf, D.A., 2003. BTB/POZ domain proteins are
859 putative substrate adaptors for cullin 3 ubiquitin ligases. Mol Cell 12, 783–790.
860
861 Godt, D., Couderc, J.L., Cramton, S.E., Laski, F.A., 1993. Pattern formation in the limbs of
862 Drosophila: bric à brac is expressed in both a gradient and a wave-like pattern and is
863 required for specification and proper segmentation of the tarsus. Development 119, 799–812.
864
865 Groth, A.C., Fish, M., Nusse, R., Calos, M.P., 2004. Construction of transgenic Drosophila by
866 using the site-specific integrase from phage phiC31. Genetics 166, 1775–1782.
867
868 Harrison, S.D., Travers, A.A., 1990. The tramtrack gene encodes a Drosophila finger protein that
869 interacts with the ftz transcriptional regulatory region and shows a novel embryonic
870 expression pattern. EMBO J 9, 207–216.
871
872 Hudson, A.M., Cooley, L., 2010. Drosophila Kelch functions with Cullin-3 to organize the ring
873 canal actin cytoskeleton. J Cell Biol 188, 29–37. doi:10.1083/jcb.200909017
874
875 Iannacone, M.J., Beets, I., Lopes, L.E., Churgin, M.A., Fang-Yen, C., Nelson, M.D., Schoofs, L.,
876 Raizen, D.M., 2017. The RFamide receptor DMSR-1 regulates stress-induced sleep in C.
877 elegans. Elife 6, 377. doi:10.7554/eLife.19837
878
879 Ji, A.X., Chu, A., Nielsen, T.K., Benlekbir, S., Rubinstein, J.L., Privé, G.G., 2015. Structural
880 insights into KCTD protein assembly and Cullin3 recognition. J Mol Biol.
881 doi:10.1016/j.jmb.2015.08.019
882
883 Ji, A.X., Privé, G.G., 2013. Crystal Structure of KLHL3 in Complex with Cullin3. PLoS ONE 8,
884 e60445. doi:10.1371/journal.pone.0060445

885
886 Kasahara, K., Kawakami, Y., Kiyono, T., Yonemura, S., Kawamura, Y., Era, S., Matsuzaki, F.,
887 Goshima, N., Inagaki, M., 2014. Ubiquitin-proteasome system controls ciliogenesis at the
888 initial step of axoneme extension. Nat Comms 5, 5081. doi:10.1038/ncomms6081
889
890 Kim, E.-J., Kim, S.-H., Jin, X., Jin, X., Kim, H., 2017. KCTD2, an adaptor of Cullin3 E3
891 ubiquitin ligase, suppresses gliomagenesis by destabilizing c-Myc. Cell Death Differ 24,
892 649–659. doi:10.1038/cdd.2016.151
893
894 Koh, K., Joiner, W.J., Wu, M.N., Yue, Z., Smith, C.J., Sehgal, A., 2008. Identification of
895 SLEEPLESS, a sleep-promoting factor. Science 321, 372–376. doi:10.1126/science.1155942
896
897 Li, Q., Kellner, D.A., Hatch, H.A.M., Yumita, T., Sanchez, S., Machold, R.P., Frank, C.A.,
898 Stavropoulos, N., 2017. Conserved properties of Drosophila Insomniac link sleep regulation
899 and synaptic function. PLoS Genet 13, e1006815. doi:10.1371/journal.pgen.1006815
900
901 Li, Q., Stavropoulos, N., 2016. Evaluation of Ligand-Inducible Expression Systems for
902 Conditional Neuronal Manipulations of Sleep in Drosophila. G3: Genes | Genomes |
903 Genetics 6, 3351–3359. doi:10.1534/g3.116.034132
904
905 Lin, D.M., Goodman, C.S., 1994. Ectopic and increased expression of Fasciclin II alters
906 motoneuron growth cone guidance. Neuron 13, 507–523.
907
908 McGourty, C.A., Akopian, D., Walsh, C., Gorur, A., Werner, A., Schekman, R., Bautista, D.,
909 Rape, M., 2016. Regulation of the CUL3 Ubiquitin Ligase by a Calcium-Dependent Co-
910 adaptor. Cell 167, 525–538.e14. doi:10.1016/j.cell.2016.09.026
911
912 Mencacci, N.E., Rubio-Agusti, I., Zdebik, A., Asmus, F., Ludtmann, M.H.R., Ryten, M.,
913 Plagnol, V., Hauser, A.-K., Bandres-Ciga, S., Bettencourt, C., Forabosco, P., Hughes, D.,
914 Soutar, M.M.P., Peall, K., Morris, H.R., Trabzuni, D., Tekman, M., Stanescu, H.C., Kleta,
915 R., Carecchio, M., Zorzi, G., Nardocci, N., Garavaglia, B., Lohmann, E., Weissbach, A.,
916 Klein, C., Hardy, J., Pittman, A.M., Foltynie, T., Abramov, A.Y., Gasser, T., Bhatia, K.P.,
917 Wood, N.W., 2015. A missense mutation in KCTD17 causes autosomal dominant
918 myoclonus-dystonia. American journal of human genetics 96, 938–947.
919 doi:10.1016/j.ajhg.2015.04.008
920
921 Papazian, D.M., Schwarz, T.L., Tempel, B.L., Jan, Y.N., Jan, L.Y., 1987. Cloning of genomic
922 and complementary DNA from Shaker, a putative potassium channel gene from Drosophila.
923 Science 237, 749–753. doi:10.1126/science.2441470
924
925 Pfeiffenberger, C., Allada, R., 2012. Cul3 and the BTB adaptor insomniac are key regulators of
926 sleep homeostasis and a dopamine arousal pathway in Drosophila. PLoS Genet 8, e1003003.
927 doi:10.1371/journal.pgen.1003003
928
929 Pintard, L., Willis, J.H., Willems, A., Johnson, J.-L.F., Srayko, M., Kurz, T., Glaser, S., Mains,
930 P.E., Tyers, M., Bowerman, B., Peter, M., 2003. The BTB protein MEL-26 is a substrate-

931 specific adaptor of the CUL-3 ubiquitin-ligase. Nature 425, 311–316.
932 doi:10.1038/nature01959
933
934 Pongs, O., Kecskemethy, N., Müller, R., Krah-Jentgens, I., Baumann, A., Kiltz, H.H., Canal, I.,
935 Llamazares, S., Ferrus, A., 1988. Shaker encodes a family of putative potassium channel
936 proteins in the nervous system of Drosophila. EMBO J 7, 1087–1096.
937
938 Rogulja, D., Young, M.W., 2012. Control of sleep by cyclin A and its regulator. Science 335,
939 1617–1621. doi:10.1126/science.1212476
940
941 Ryder, E., Blows, F., Ashburner, M., Bautista-Llacer, R., Coulson, D., Drummond, J., Webster,
942 J., Gubb, D., Gunton, N., Johnson, G., O'kane, C.J., Huen, D., Sharma, P., Asztalos, Z.,
943 Baisch, H., Schulze, J., Kube, M., Kittlaus, K., Reuter, G., Maroy, P., Szidonya, J.,
944 Rasmuson-Lestander, A., Ekström, K., Dickson, B., Hugentobler, C., Stocker, H., Hafen, E.,
945 Lepesant, J.A., Pflugfelder, G., Heisenberg, M., Mechler, B., Serras, F., Corominas, M.,
946 Schneuwly, S., Preat, T., Roote, J., Russell, S., 2004. The DrosDel collection: a set of P-
947 element insertions for generating custom chromosomal aberrations in Drosophila
948 melanogaster. Genetics 167, 797–813. doi:10.1534/genetics.104.026658
949
950 Schwenk, J., Metz, M., Zolles, G., Turecek, R., Fritzius, T., Bildl, W., Tarusawa, E., Kulik, A.,
951 Unger, A., Ivankova, K., Seddik, R., Tiao, J.Y., Rajalu, M., Trojanova, J., Rohde, V.,
952 Gassmann, M., Schulte, U., Fakler, B., Bettler, B., 2010. Native GABA(B) receptors are
953 heteromultimers with a family of auxiliary subunits. Nature 465, 231–235.
954 doi:10.1038/nature08964
955
956 Singh, C., Rihel, J., Prober, D.A., 2017. Neuropeptide Y Regulates Sleep by Modulating
957 Noradrenergic Signaling. Curr Biol 27, 3796–3811.e5. doi:10.1016/j.cub.2017.11.018
958
959 Stavropoulos, N., Young, M.W., 2011. insomniac and Cullin-3 regulate sleep and wakefulness in
960 Drosophila. Neuron 72, 964–976. doi:10.1016/j.neuron.2011.12.003
961
962 Stogios, P.J., Downs, G.S., Jauhal, J.J.S., Nandra, S.K., Privé, G.G., 2005. Sequence and
963 structural analysis of BTB domain proteins. Genome Biol 6, R82. doi:10.1186/gb-2005-6-
964 10-r82
965
966 Toda, H., Williams, J.A., Gulledge, M., Sehgal, A., 2019. A sleep-inducing gene, nemuri, links
967 sleep and immune function in Drosophila. Science 363, 509–515.
968 doi:10.1126/science.aat1650
969
970 Wee, S., Geyer, R.K., Toda, T., Wolf, D.A., 2005. CSN facilitates Cullin-RING ubiquitin ligase
971 function by counteracting autocatalytic adapter instability. Nat Cell Biol 7, 387–391.
972 doi:10.1038/ncb1241
973
974 Wei, A., Covarrubias, M., Butler, A., Baker, K., Pak, M., Salkoff, L., 1990. K+ current diversity
975 is produced by an extended gene family conserved in Drosophila and mouse. Science 248,
976 599–603. doi:10.1126/science.2333511

977
978 Wu, M., Robinson, J.E., Joiner, W.J., 2014. SLEEPLESS is a bifunctional regulator of
979 excitability and cholinergic synaptic transmission. Curr Biol 24, 621–629.
980 doi:10.1016/j.cub.2014.02.026
981
982 Wu, M.N., Joiner, W.J., Dean, T., Yue, Z., Smith, C.J., Chen, D., Hoshi, T., Sehgal, A., Koh, K.,
983 2010. SLEEPLESS, a Ly-6/neurotoxin family member, regulates the levels, localization and
984 activity of Shaker. Nat Neurosci 13, 69–75. doi:10.1038/nn.2454
985
986 Xu, L., Wei, Y., Reboul, J., Vaglio, P., Shin, T.-H., Vidal, M., Elledge, S.J., Harper, J.W., 2003.
987 BTB proteins are substrate-specific adaptors in an SCF-like modular ubiquitin ligase
988 containing CUL-3. Nature 425, 316–321. doi:10.1038/nature01985
989
990 Zhang, D.D., Lo, S.-C., Sun, Z., Habib, G.M., Lieberman, M.W., Hannink, M., 2005.
991 Ubiquitination of Keap1, a BTB-Kelch substrate adaptor protein for Cul3, targets Keap1 for
992 degradation by a proteasome-independent pathway. J Biol Chem 280, 30091–30099.
993 doi:10.1074/jbc.M501279200
994

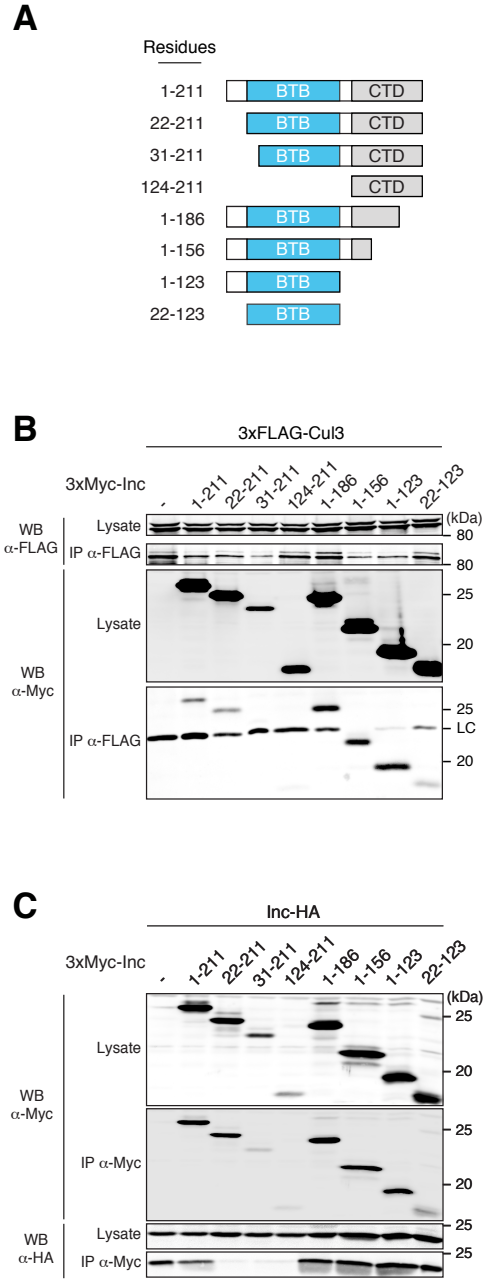
A
Residues
1-211
22-211
31-211
124-211
1-186
1-156
1-123
22-123
BTB
CTD
B
3xFLAG-Cul3
3xMyc-Inc
-
1-211
22-211
31-211
124-211
1-186
1-156
1-123
22-123
(kDa)
WB
α-FLAG
Lysate
IP α-FLAG
80
80
WB
α-Myc
Lysate
IP α-FLAG
25
20
25
LC
20
C
Inc-HA
3xMyc-Inc
WB
α-Myc
Lysate
IP α-Myc
WB
α-HA
Lysate
IP α-Myc

Figure 1

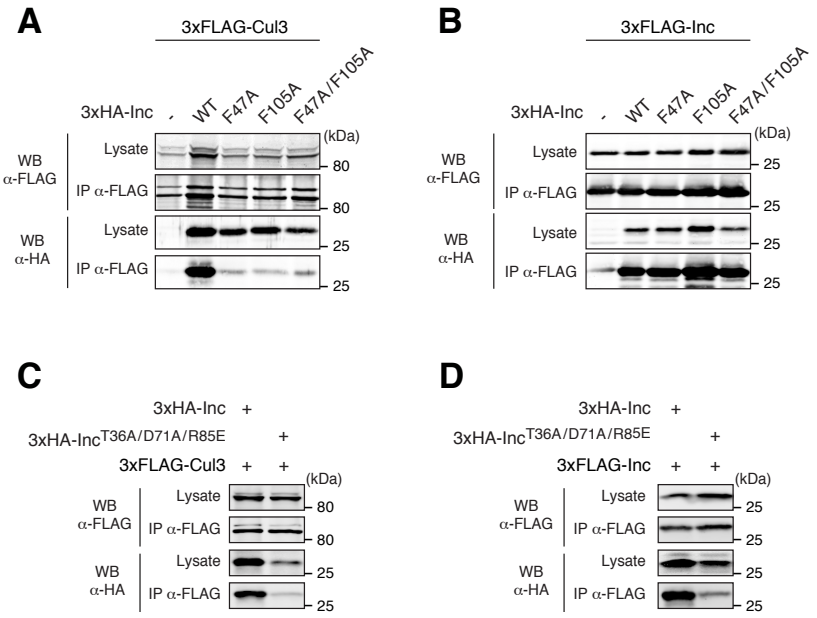
A
3xFLAG-Cul3
3xHA-Inc
WT
F47A
F105A
F47A/F105A
(kDa)
WB α-FLAG
Lysate
IP α-FLAG
80
80
WB α-HA
Lysate
IP α-FLAG
25
25
B
3xFLAG-Inc
3xHA-Inc
WT
F47A
F105A
F47A/F105A
(kDa)
WB α-FLAG
Lysate
IP α-FLAG
25
25
WB α-HA
Lysate
IP α-FLAG
25
25
C
3xHA-Inc +
3xHA-IncT36A/D71A/R85E +
3xFLAG-Cul3 + +
(kDa)
WB α-FLAG
Lysate
IP α-FLAG
80
80
WB α-HA
Lysate
IP α-FLAG
25
25
D
3xHA-Inc +
3xHA-IncT36A/D71A/R85E +
3xFLAG-Inc + +
(kDa)
WB α-FLAG
Lysate
IP α-FLAG
25
25
WB α-HA
Lysate
IP α-FLAG
25
25

Figure 2

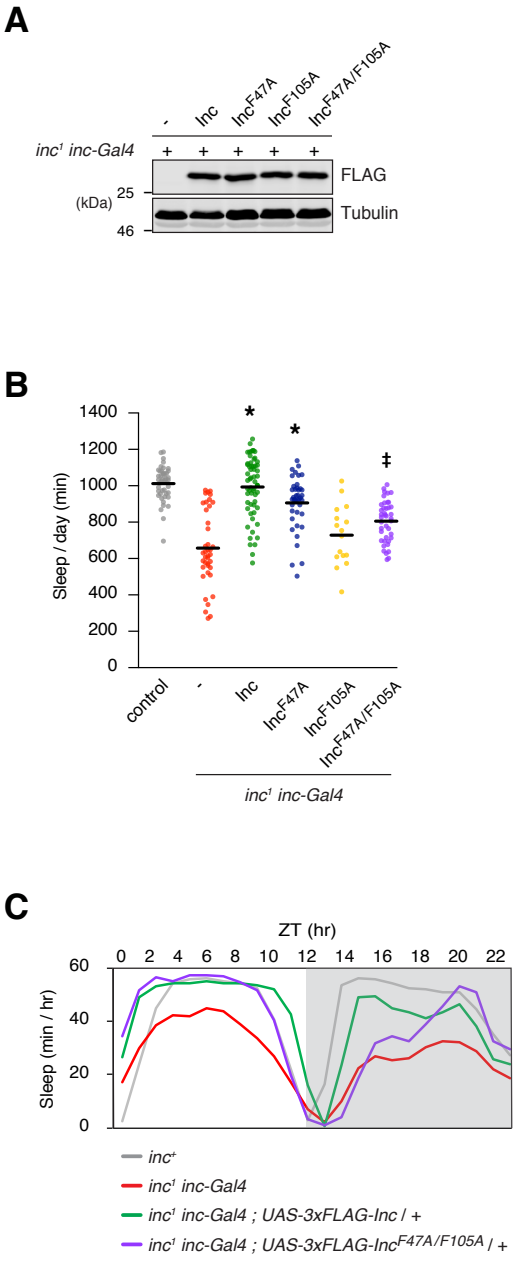
A
-
Inc
IncF47A
IncF105A
IncF47A/F105A
inc1 inc-Gal4
+ + + + +
FLAG
(kDa)
25
Tubulin
46
B
Sleep / day (min)
1400
1200
1000
800
600
400
200
0
*
*
‡
control
-
Inc
IncF47A
IncF105A
IncF47A/F105A
inc1 inc-Gal4
C
ZT (hr)
0 2 4 6 8 10 12 14 16 18 20 22
Sleep (min / hr)
60
40
20
0
inc+
inc1 inc-Gal4
inc1 inc-Gal4 ; UAS-3xFLAG-Inc / +
inc1 inc-Gal4 ; UAS-3xFLAG-IncF47A/F105A / +

Figure 3

A

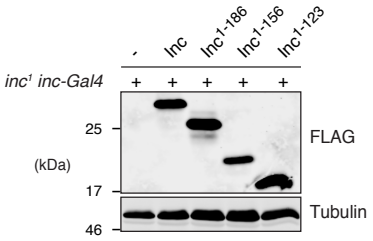
-
Inc
Inc1-186
Inc1-156
Inc1-123
inc1 inc-Gal4
+ + + + +
25
(kDa)
17
46
FLAG
Tubulin

B

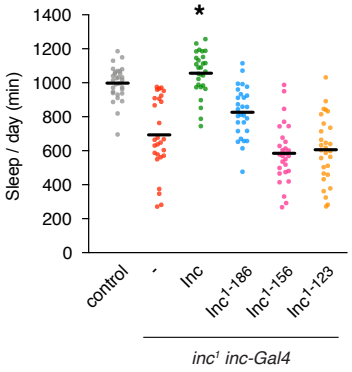
1400
1200
1000
800
600
400
200
0
Sleep / day (min)
*
control
-
Inc
Inc1-186
Inc1-156
Inc1-123
inc1 inc-Gal4

C

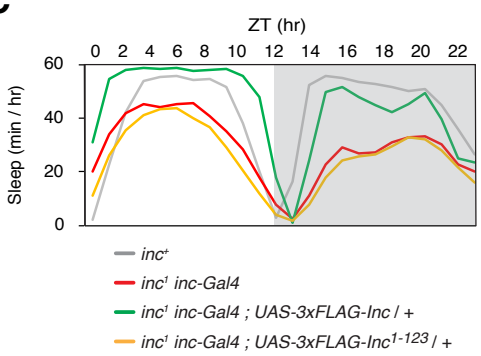
ZT (hr)
0 2 4 6 8 10 12 14 16 18 20 22
60
40
20
0
Sleep (min / hr)
inc+
inc1 inc-Gal4
inc1 inc-Gal4 ; UAS-3xFLAG-Inc / +
inc1 inc-Gal4 ; UAS-3xFLAG-Inc1-123 / +

Figure 4

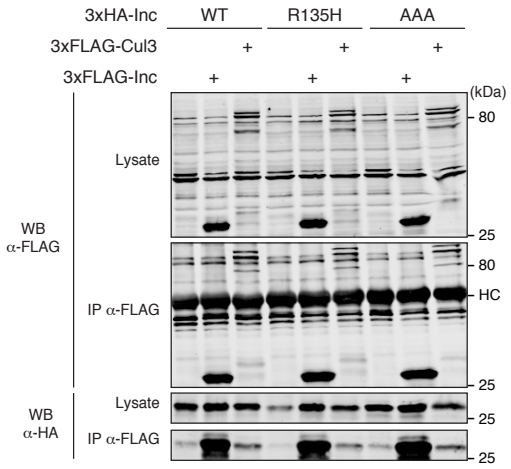
3xHA-Inc
WT
R135H
AAA
3xFLAG-Cul3
+
+
+
3xFLAG-Inc
+
+
+
(kDa)
80
Lysate
25
WB
α-FLAG
80
HC
IP α-FLAG
25
Lysate
25
WB
α-HA
IP α-FLAG
25

Figure 5

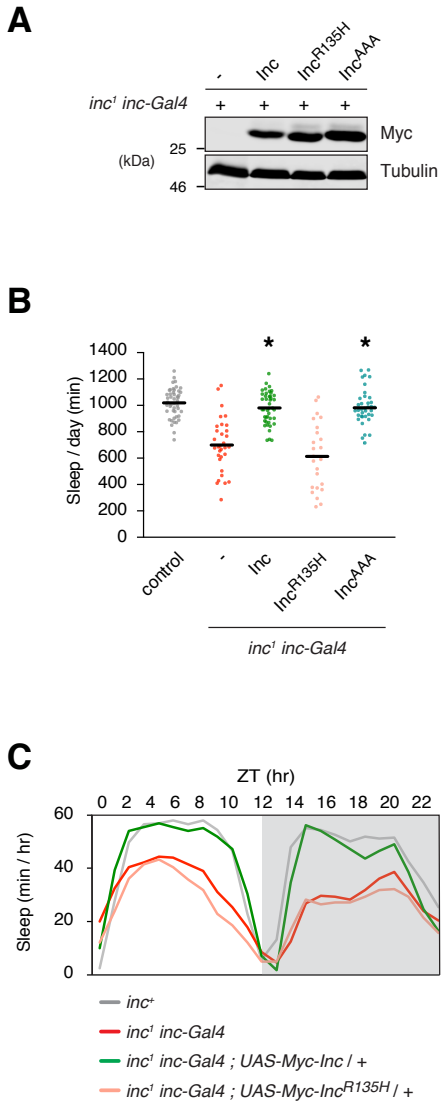
A
-
Inc
IncR135H
IncAAA
inc1 inc-Gal4
+ + + +
Myc
Tubulin
(kDa)
25
46
B
Sleep / day (min)
1400
1200
1000
800
600
400
200
0
*
*
control
-
Inc
IncR135H
IncAAA
inc1 inc-Gal4
C
ZT (hr)
0 2 4 6 8 10 12 14 16 18 20 22
Sleep (min / hr)
60
40
20
0
inc+
inc1 inc-Gal4
inc1 inc-Gal4 ; UAS-Myc-Inc / +
inc1 inc-Gal4 ; UAS-Myc-IncR135H / +

Figure 6

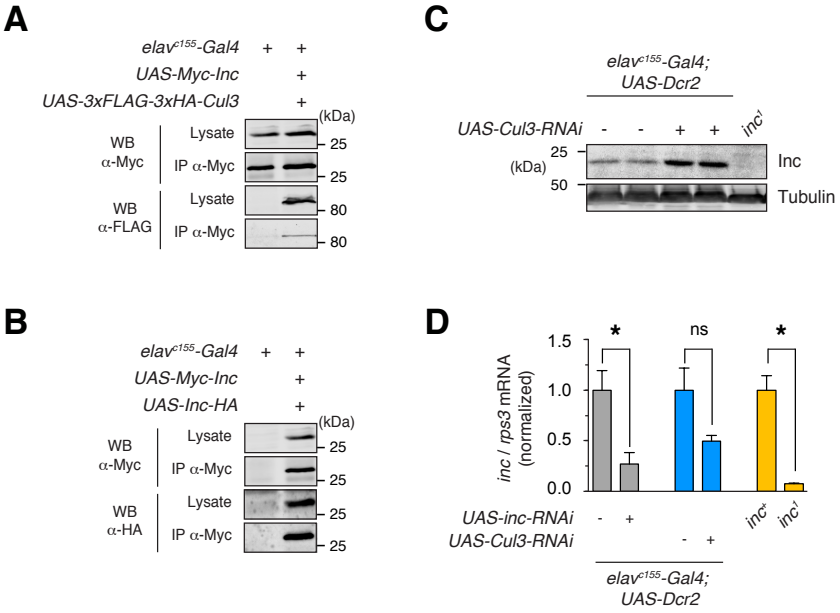
A
elavc155-Gal4 + +
UAS-Myc-Inc +
UAS-3xFLAG-3xHA-Cul3 +
(kDa)
WB α-Myc
Lysate
IP α-Myc
25
25
WB α-FLAG
Lysate
IP α-Myc
80
80
B
elavc155-Gal4 + +
UAS-Myc-Inc +
UAS-Inc-HA +
(kDa)
WB α-Myc
Lysate
IP α-Myc
25
25
WB α-HA
Lysate
IP α-Myc
25
25
C
elavc155-Gal4; UAS-Dcr2
UAS-Cul3-RNAi - - + + inc1
(kDa)
25
50
Inc
Tubulin
D
inc / rps3 mRNA (normalized)
1.5
1.0
0.5
0.0
*
ns
*
UAS-inc-RNAi - +
UAS-Cul3-RNAi - +
inc+
inc1
elavc155-Gal4; UAS-Dcr2

Figure 7

	Inc mutant	Inc-Inc	Inc-Cul3	Inc stability
1	Inc^{F47A}	n.c.	Strongly reduced	n.c.
2	Inc^{R50E}	Reduced	Reduced	n.c.
3	Inc^{D57A}	n.c.	n.c.	n.c.
4	Inc^{D61A}	n.c.	n.c.	n.c.
5	Inc^{E104K}	n.c.	n.c.	n.c.
6	Inc^{F105A}	n.c.	Strongly reduced	n.c.
7	Inc^{Y106A}	n.c.	n.c.	n.c.
8	Inc^{N107A}	n.c.	n.c.	n.c.
9	$Inc^{F47A/F105A}$	n.c.	Strongly reduced	n.c.

n.c. (no change)

Table 1

	Inc mutant	Inc-Inc	Inc-Cul3	Inc stability
1	$Inc^{T36A/D71A/R85E}$	Strongly reduced	Reduced	Strongly reduced
2	$Inc^{T36A/D71A}$	n.c.	n.c.	n.c.
3	$Inc^{D71A/R85E}$	n.c.	Reduced	Strongly reduced
4	$Inc^{D73A/N82A}$	n.c.	n.c.	n.c.
5	$Inc^{K88D/E101K}$	n.c.	Reduced	n.c.
6	Inc^{T36A}	n.c.	n.c.	n.c.

n.c. (no change)

Table 2

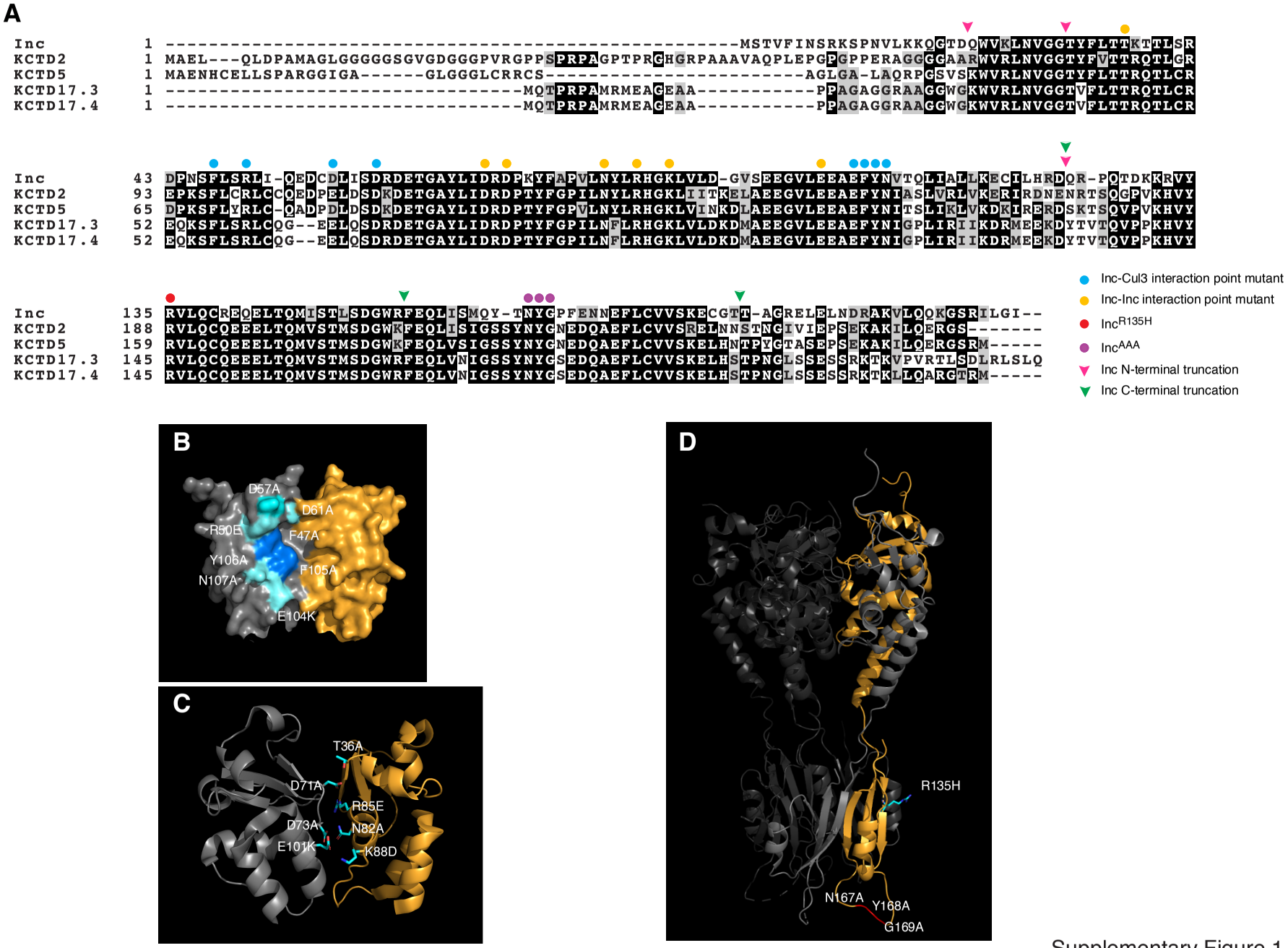

Supplementary Figure 1

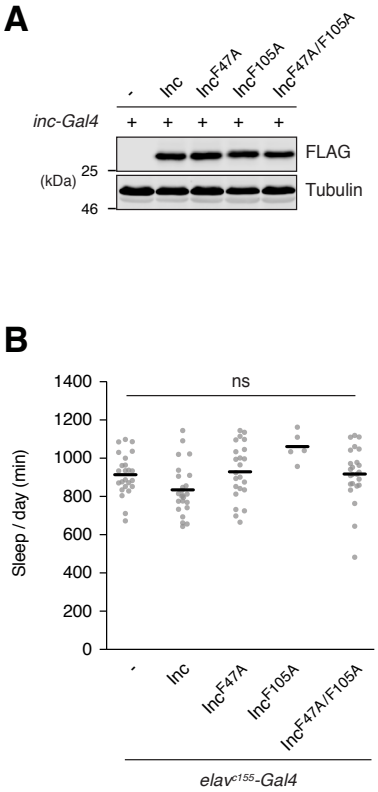

Supplementary Figure 2

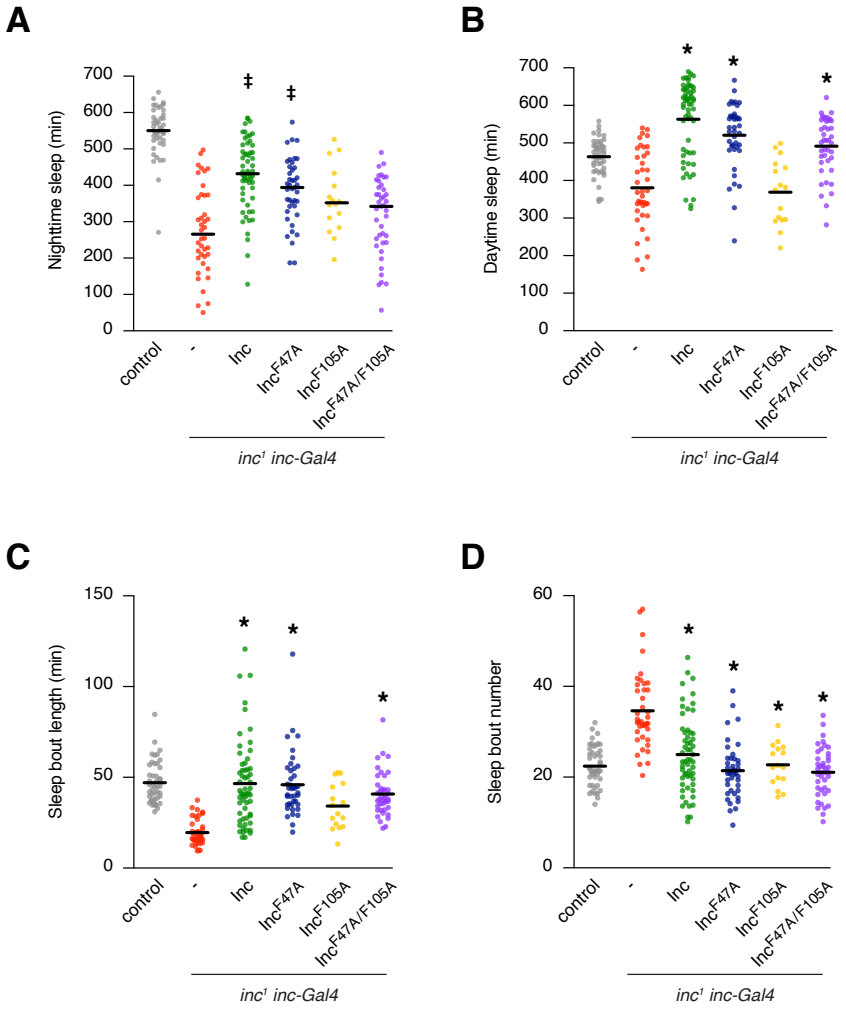

Supplementary Figure 3

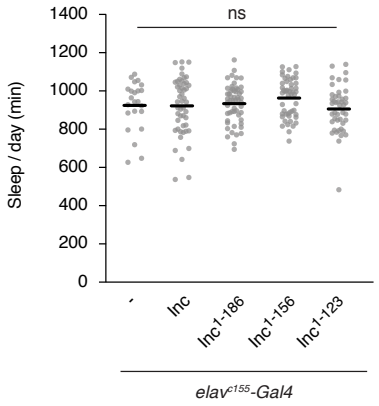

Supplementary Figure 4

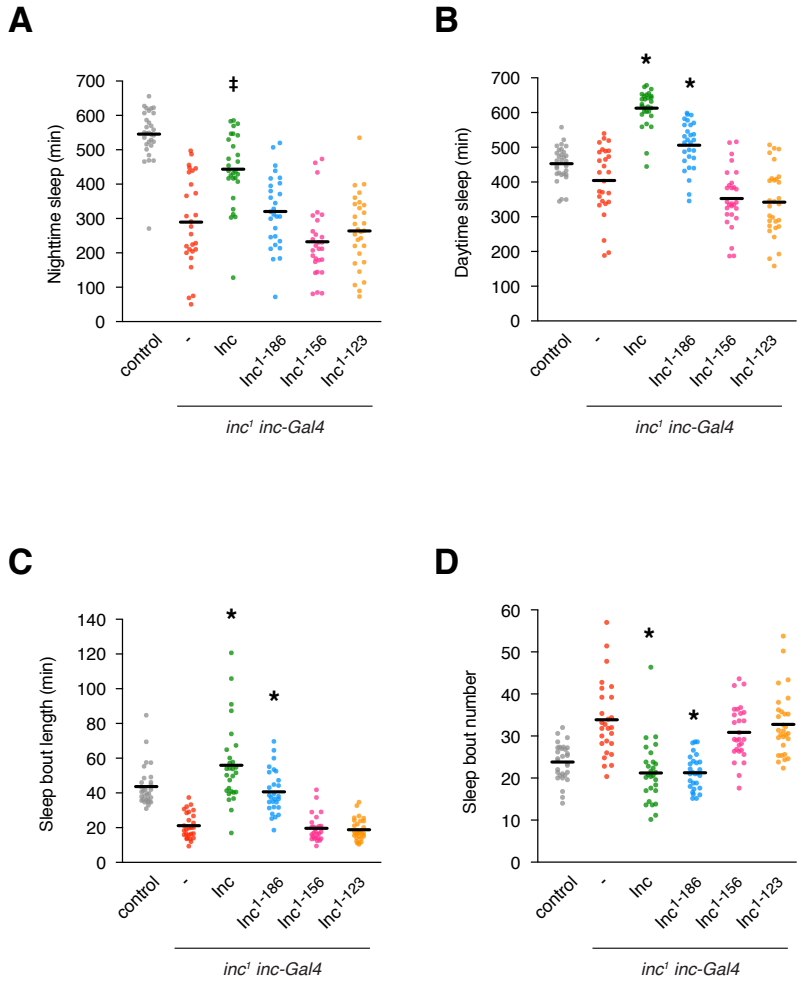

Supplementary Figure 5

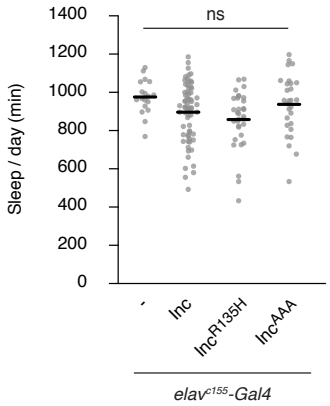

Supplementary Figure 6

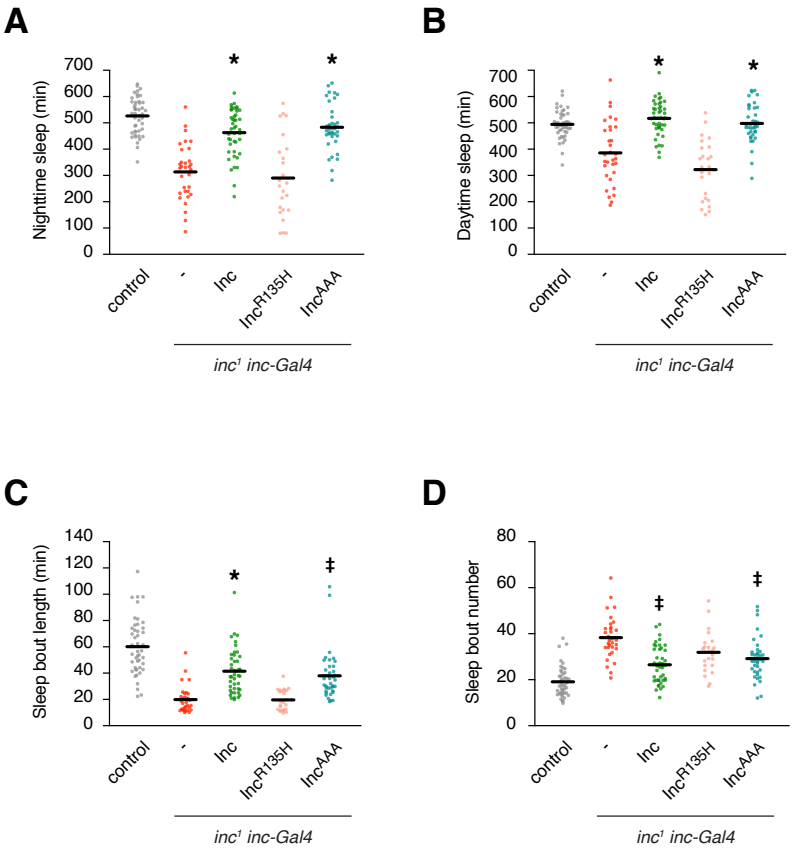

Supplementary Figure 7